Ambient Femtosecond Laser Vaporization and Nanosecond Laser Desorption Electrospray Ionization Mass Spectrometry

Paul Flanigan and Robert Levis

Center for Advanced Photonics Research, Department of Chemistry, Temple University, Philadelphia, Pennsylvania 19122; email: paul.flanigan@temple.edu, rjlevis@temple.edu

Annu. Rev. Anal. Chem. 2014. 7:229–56

The *Annual Review of Analytical Chemistry* is online at anchem.annualreviews.org

This article's doi: 10.1146/annurev-anchem-071213-020343

Keywords

femtosecond laser vaporization, nanosecond laser desorption, electrospray postionization, ambient mass spectrometry, laser electrospray mass spectrometry

Abstract

Recent investigations of ambient laser-based transfer of molecules into the gas phase for subsequent mass spectral analysis have undergone a renaissance resulting from the separation of vaporization and ionization events. Here, we seek to provide a snapshot of recent femtosecond (fs) duration laser vaporization and nanosecond (ns) duration laser desorption electrospray ionization mass spectrometry experiments. The former employs pulse durations of <100 fs to enable matrix-free laser vaporization with little or no fragmentation. When coupled to electrospray ionization, femtosecond laser vaporization provides a universal, rapid mass spectral analysis method requiring no sample workup. Remarkably, laser pulses with intensities exceeding 10^{13} W cm^{-2} desorb intact macromolecules, such as proteins, and even preserve the condensed phase of folded or unfolded protein structures according to the mass spectral charge state distribution, as demonstrated for cytochrome *c* and lysozyme. Because of the ability to vaporize and ionize multiple components from complex mixtures for subsequent analysis, near perfect classification of explosive formulations, plant tissue phenotypes, and even the identity of the manufacturer of smokeless powders can be determined by multivariate statistics. We also review the more mature field of nanosecond laser desorption for ambient mass spectrometry, covering the wide range of systems analyzed, the need for resonant absorption, and the spatial imaging of complex systems like tissue samples.

LASER VAPORIZATION FOR MASS SPECTROMETRY

The genesis of laser mass spectrometry occurred shortly after the discovery of the ruby laser in 1960 (1), with early work involving both gas phase ionization via resonance-enhanced multiphoton ionization (2) and ablation of solids coupled to time-of-flight mass spectrometry, which evolved into the laser microprobe (3). The realization that lasers could be used to both desorb and ionize molecules was pioneered in the early 1980s along with a number of other energy deposition and ionization sources, including fast atom bombardment (4), secondary ion mass spectrometry (5), and plasma desorption mass spectrometry (6) sources. A major goal during this period was to break the barrier for the mass spectral analysis of macromolecules with masses greater than ~1 kDa. Two approaches ultimately resolved the challenge, electrospray ionization mass spectrometry (ESI-MS) (7, 8) and laser desorption (9). In an electrospray experiment, the molecule is sprayed into the gas phase in a charged droplet, and when the solvent evaporates, the charged analyte is available for mass analysis. In the laser desorption experiment, Tanaka et al. (9) discovered that a glycerol solution containing colloidal cobalt would absorb a pulsed laser in a manner that resulted in the transfer and ionization of a protein (lysozyme) from the condensed phase into the gas phase. Hillenkamp and coworkers (10–12) reported that a small organic acid matrix could both solvate the biomolecule and absorb the laser radiation to enable desorption. Hence, the experiment known as matrix-assisted laser desorption/ionization (MALDI) was realized.

Although MALDI and ESI have grown to become the dominant mass spectral techniques for macromolecule analysis, both have advantages and shortcomings that make them complementary techniques. For example, in the analysis of tissue samples, ESI requires extensive sample preparation (homogenization and separation steps) that results in the selective isolation of a particular class of molecules with loss of information regarding the remaining molecules in the system. To perform direct, spatially resolved analysis is challenging for ESI, and the desorption electrospray ionization (DESI) experiment has made strides toward resolving this challenge (13). MALDI, by contrast, is particularly well suited for spatially resolved analysis but initially required tissue states to be altered by drying or freezing prior to transfer into the high-vacuum system. About 10 years after MALDI and ESI were established, atmospheric pressure (AP)-MALDI was achieved (14, 15). AP-MALDI demonstrated less fragmentation caused by collisional cooling in the gas phase (15, 16), was amenable to mass analyzers other than time-of-flight (17, 18), and because of fewer sample preparation steps, enabled spatially resolved imaging of tissue and other biological samples with <10-μm resolution (19–21). AP-MALDI experiments using an IR laser (AP-IR-MALDI) do not require matrix molecules in the analysis of water-rich tissue samples as the laser beam couples to water in the sample (22, 23). The initial low sensitivity from ion losses at the atmospheric pressure-to-vacuum interface of the mass spectrometer inlet (15, 24) and discrimination against higher mass-to-charge (m/z) ions (>3,000) owing to recombination in the plume (22) have been improved through analysis in the transmission mode in a field-free region (25–27).

Separating vaporization and ionization into two distinct processes enables measurements that cannot be performed using either ESI-MS or MALDI alone. This review focuses on recent investigations of laser-based mass spectrometry with an emphasis on laser release of molecules from the condensed phase at atmospheric pressure for subsequent ionization and mass spectral analysis using electrospray ionization. We first thoroughly describe femtosecond laser vaporization with electrospray postionization, which is called laser electrospray mass spectrometry (LEMS), as this is the chief focus of the review. Then, we comprehensively detail related laser-electrospray hybrid techniques using nanosecond lasers, with particular emphasis on electrospray-assisted laser desorption/ionization (ELDI), matrix-assisted laser desorption electrospray ionization (MALDESI), and laser ablation electrospray ionization (LAESI). Finally, we review single-step ambient laser

desorption and ionization mass spectral techniques. Comprehensive overviews of ambient pressure mass spectrometry and laser-based imaging methods have been previously published (28–41).

TWO-STEP METHODS USING LASER DESORPTION AND ELECTROSPRAY POSTIONIZATION

Methods for separating the desorption and ionization processes to prepare nonvolatile analytes for mass spectral analysis now constitute an important research focus. The goal is to provide a greater degree of control over each step to enhance analytical capabilities. The process of separating desorption from the ionization steps can be accomplished by several methods. Early attempts employing laser postionization following laser desorption were largely limited to smaller molecules because of rapid photophysical transfer of laser excitation energy to internal modes of the analyte (42). In 2004, the atmospheric pressure mass spectrometry revolution was started by DESI (13), and after this breakthrough, many ESI-related mass spectral techniques were developed for ambient surface analysis. The combination of laser desorption with electrospray postionization in particular provides several benefits, including atmospheric pressure analysis, direct sampling, enhanced quantitative analysis, and spatially resolved analysis. The latter three capabilities are difficult with conventional electrospray techniques. The general depiction for this type of hybrid mass analysis technique is shown in **Figure 1** with tables listing key parameters and results for the four major hybrid techniques discussed below.

Laser Electrospray Mass Spectrometry

Femtosecond (fs) laser vaporization has been explored recently as a universal means to transfer molecules into the gas phase for atmospheric pressure mass spectrometry (43). Femtosecond laser excitation has a long history in the field of mass spectrometry and initially was employed as a means to ionize gas phase molecules without tuning to a specific resonance (44). Femtosecond duration laser pulses directly couple into the molecular system through multiphoton, nonresonant absorption (44–46). At the laser intensities employed to drive ionization through nonresonant multiphoton excitation ($\sim 10^{13-14}$ W cm^{-2}), one anticipates considerable fragmentation of the excited molecule. In fact, in many instances, the fragmentation is limited with the parent molecular ion dominating the mass spectrum. This occurs because the ~50-fs pulse is shorter than the typical molecular rearrangement time (47), initiating ladder climbing to rapidly induce ionization instead of ladder switching mechanisms during which fragmentation results. Conversely, nonresonant nanosecond laser pulses cause much more fragmentation at similar intensities (46, 48–50) because of the ladder switching mechanism. The high photon intensity reached during femtosecond irradiation also enables tunnel ionization and impulsive vibrational excitation (51–53); alternative mechanisms are not considered here.

The use of a femtosecond laser as a means of coupling directly into a molecular system for its release into the gas phase has precedent in investigations of the vaporization of cryogenic films of small molecules (54–56). A comparison of femtosecond and picosecond duration pulses for vaporization showed a decrease in the yield of vaporized molecules with increasing thickness of a benzene multilayer for the picosecond duration pulse (54). This was attributed to the picosecond laser pulses depositing energy into the substrate to enable vaporization, and this dissipated with increasing film thickness. In the case of femtosecond duration vaporization of the cryogenic multilayers, the desorption yield monotonically increased with multilayer thickness, suggesting that the femtosecond laser energy coupled directly into the molecules. A comparison of femtosecond and nanosecond laser ablation revealed that the latter caused thermal damage to a solid substrate

Laser properties

Technique	Acronym	Pulse width	Laser light, wavelength	Pulse energy	Spatial resolution	Incidence angle
Laser electrospray mass spectrometry	LEMS	70 fs	N-IR, 800 nm	0.4–2.5 mJ	250 μm in diameter	45°
Electrospray-assisted laser desorption/ionization	ELDI	4 ns	UV, 337 nm N-IR, 1064 nm	20–150 μJ	100 μm^2	45°
	IR-ELDI	7 ns	SW-IR, 2.94 μm	150 μJ	400 μm in diameter	90°
Matrix-assisted laser desorption electrospray ionization	MALDESI IR-MALDESI	4 ns 7 ns	UV, 337/349 nm SW-IR, 2.94 μm	0.1–1.5 mJ	45 μm in diameter	45°
Laser ablation electrospray ionization	LAESI	7 ns	SW-IR, 2.94 μm	0.1–3 mJ	30 μm in diameter	90°

Electrospray conditions

Technique	ESI or nanoESI	Flow rate	Height above sample
LEMS	ESI	3.0 μL/min	6.5 mm
ELDI	ESI	2.5 μL/min	3 mm
MALDESI	nanoESI	400 nL/min	5.5 mm
LAESI	nanoESI	200 nL/min	Up to 15 mm

Sample stage

Technique	Stage voltage
LEMS	–2,000 V
ELDI	0 V
MALDESI	550 V
LAESI	0 V

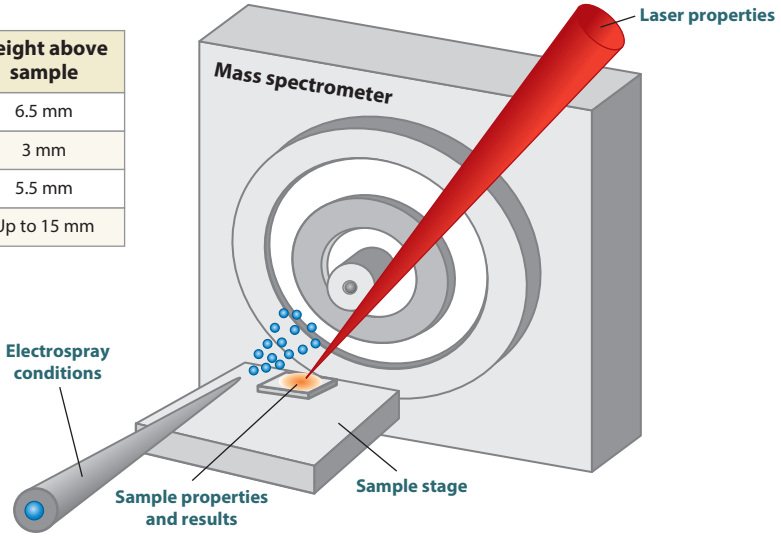

Sample properties and results

Technique	Sample requirements	Sample state	Highest mass	Detection limit, sample	Dynamic range
LEMS	None	Solid, liquid	45 kDa	17 pmol, lysozyme 2 decades > ESI	2.5 decades
ELDI	None for dried, matrix enhances signal for liquid	Solid, liquid	66 kDa	30 fmol, cytochrome *c*	4 decades
MALDESI	Organic matrix or water rich for IR-MALDESI	Solid, liquid	17 kDa	10 amol, cytochrome *c*	N/A
LAESI	Water-rich sample	Solid, liquid	66 kDa	600 amol, verapamil	6 decades

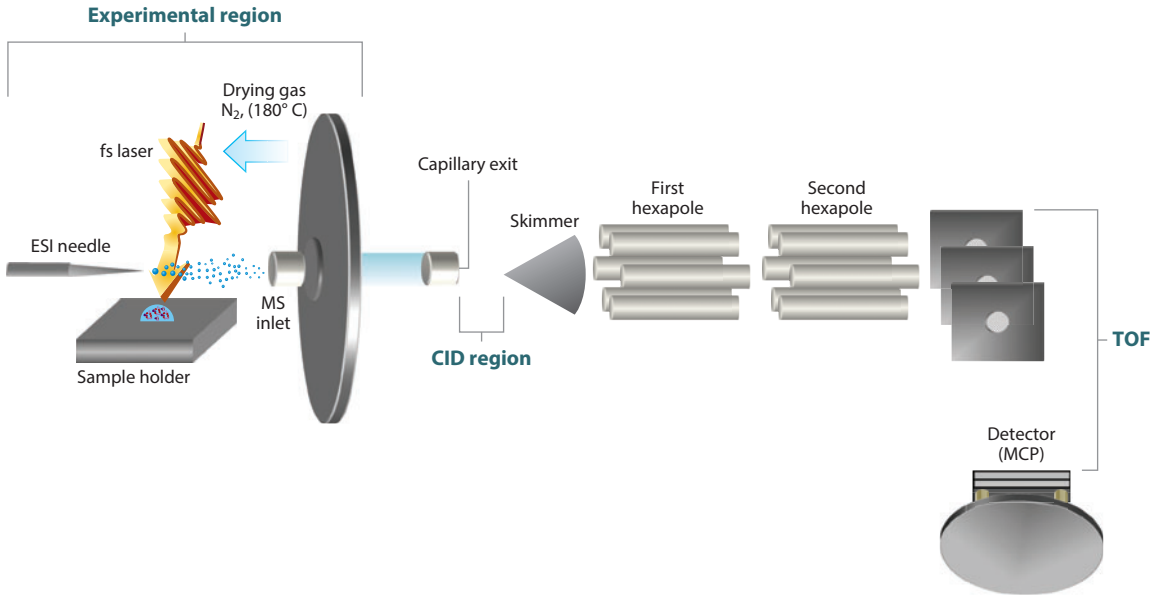

Figure 2

Schematic of the instrumental setup for laser electrospray mass spectrometry experiments. The experimental region is where the laser vaporization, electrospray postionization, and transfer into the mass spectrometer are performed. The in-source collision-induced dissociation (CID) region is where fragmentation occurs in the mass spectrometer at energies that are selected by varying the capillary exit voltage. Then, the ions travel through two hexapoles to a pulsed and orthogonal extraction region, are separated by mass-to-charge ratio in a time-of-flight (TOF) tube, and are detected using microchannel plates (MCP). Other abbreviations: ESI, electrospray ionization; MS, mass spectrometer.

that did not occur in the case of femtosecond duration ablation (57). Femtosecond laser desorption also results in a lower ion yield in comparison with nanosecond lasers at similar pulse energies, as seen in MALDI investigations (58, 59). Instead of ions, neutral molecules have been shown to be the major product of nanosecond laser desorption without a matrix (60). A review of nanosecond and femtosecond laser ablation in analytical techniques has already been published (61).

In 2009, we extended the ultrafast excitation of molecules to the condensed phase and reported a new method to nonresonantly vaporize molecules using 800-nm, 70-fs laser pulses with a much higher intensity (10^{13} W cm^{-2}) (43) than the laser-electrospray hybrid experiments reviewed below in the ELDI, MALDESI, and LAESI sections. The use of femtosecond laser pulses for vaporization followed by electrospray for postionization was called LEMS, and a typical experimental apparatus is shown in **Figure 2**. In the LEMS experiment, samples in numerous states (liquid, dried, mixtures, tissue, etc.) have been vaporized and analyzed, as described later in this section. The vaporization

Figure 1

Schematic for two-step mass spectral methods using laser ablation followed by electrospray postionization. Key properties and results are shown in the respective tables. References used to create this figure include the following: LEMS (43, 63, 64, 73, 79), ELDI (81, 82, 88, 92, 93), IR-ELDI (96), MALDESI (70, 98), IR-MALDESI (71, 106), and LAESI (97, 120, 126). Abbreviations: ELDI, electrospray-assisted laser desorption/ionization; F-IR, far infrared; in diam., in diameter; IR-ELDI, infrared electrospray-assisted laser desorption/ionization; IR-MALDESI, infrared matrix-assisted laser desorption electrospray ionization; LAESI, laser ablation electrospray ionization; LEMS, laser electrospray mass spectrometry; MALDESI, matrix-assisted laser desorption electrospray ionization; N-IR, near infrared; SW-IR, shortwave infrared; UV, ultraviolet.

method appears to be universal and leads to a number of quantitative measurements of complex systems, and near perfect classification can be achieved, as has been demonstrated for different explosives and tissue types. The measurement is typically performed using ~1.5-mJ laser pulses operated at 10 Hz and focused to spot sizes ranging from 100 to 350 μm. Note that a matrix is not necessary to enable vaporization as the laser nonresonantly couples into all molecules investigated to date. The vaporized neutrals are intersected by an electrospray plume, which typically has a flow rate of 3 μL/min and is located 6.5 mm above the sample surface, and then are ionized and transferred into the spectrometer for mass analysis. Ambient mass analysis using femtosecond laser vaporization and ESI postionization was first performed for intact neutral molecules, such as pseudoproline dipeptide, protoporphorin IX, and vitamin B_{12}, with and without MALDI matrices (43). Although no matrix was necessary for mass analysis, the presence of 2,5-dihydroxybenzoic acid resulted in a minor increase in signal intensity and a decrease in fragmentation. Also when the ESI plume was not present, no ion signal was observed, suggesting that vaporization and ionization do not occur because of femtosecond-AP-MALDI processes.

Since the original report of femtosecond laser electrospray mass spectrometry, a number of other biological materials and biologically relevant compounds have been probed using that method, including pharmaceuticals (62, 63), proteins (64–66), lipids (67), whole blood (64, 67), milk (67), and tissue samples (68, 69). These molecules were successfully analyzed using LEMS without matrices. Pharmaceutical tablets were directly investigated without any workup other than placing a tablet on the sample stage. The LEMS analysis resulted in identification of active pharmaceutical ingredients and inactive ingredients for a cold/flu liquid caplet (62) and a Claritin® (loratadine) tablet (63). Dried pharmaceutical samples, such as loratadine, atenolol, and oxycodone, were vaporized from various substrates, including stainless steel, wood, glass, and fabrics, demonstrating the potential for universal vaporization, and further supporting the hypothesis that the laser couples directly into the analyte regardless of its molecular structure (63). Spatial imaging in two dimensions was demonstrated in principle in the analysis of oxycodone from a stainless steel substrate, as shown in **Figure 3**, using a ~400-μJ pulse focused to a spot size of ~250 μm in diameter as the sample was rastered using a stepper-motor-driven stage. LEMS neutral capture efficiencies (NCEs), which are the percentages of the vaporized molecules transferred from the sample substrate into the electrospray plume for mass analysis, have been as high as 2.5% (for oxycodone), demonstrating efficient vaporization by femtosecond lasers in comparison with nanosecond lasers as MALDESI reported NCE values of less than 0.02% (70), although MALDESI NCE values are most likely higher now owing to optimization of its parameters (71).

LEMS is a soft ionization technique for protein analysis that can reveal a condensed-phase structure through the distribution of charge states observed in the mass spectrum, as seen in **Figure 4**. Even though an ultraintense laser was used for release into the gas phase, the known charge-state distribution (CSD) for folded lysozyme (14.3 kDa), centered at 10+ and 9+ (72) in conventional ESI measurements, was observed (64) in the LEMS mass spectrum of aqueous lysozyme in **Figure 4*b***, demonstrating that an intense femtosecond laser pulse can transfer proteins intact from the condensed phase into the gas phase. Additional investigations revealed that the condensed-phase protein conformation is conserved during LEMS analysis even when the electrospray solvent may induce a conformational change in the protein because of pH and organic content (65). For instance, when cytochrome *c* was vaporized from an aqueous droplet at pH 3 or pH 7 into a neutral (pH 7) electrospray solution containing methanol, mass spectra were observed with the expected charge-state distributions for folded and unfolded proteins, respectively. In another example, LEMS analysis for aqueous neutral pH cytochrome *c* as a function of electrospray solvent pH revealed a CSD for folded proteins above pH 5. Conventional electrospray revealed a bimodal distribution corresponding to the unfolded and folded protein states from pH 7 to pH 4

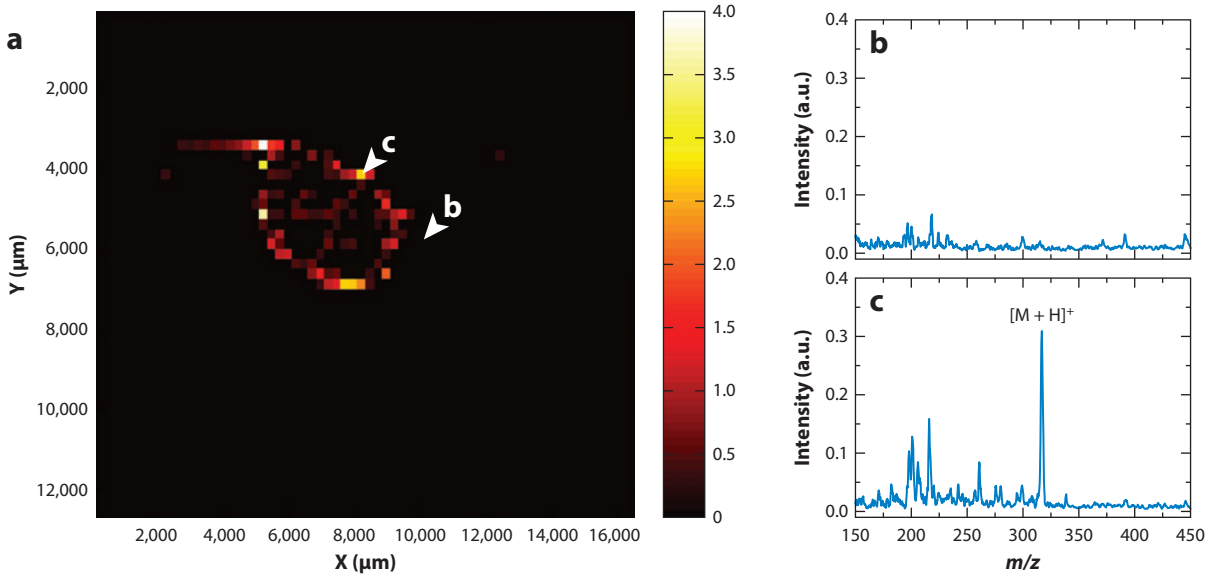

Figure 3

(*a*) Two-dimensional image of oxycodone from a stainless steel slide using laser electrospray mass spectrometry (LEMS). Representative mass spectra are shown in panel *b*, where no oxycodone is present, and in panel *c*, where a spot containing oxycodone is present. Reprinted with permission from Reference 63. Copyright 2010 American Chemical Society. Abbreviations: a.u., arbitrary unit; [M+H], protonated molecular ion; *m/z*, mass-to-charge ratio.

(lowest investigated) using buffered 1:1 (v:v) methanol:water ESI solvents. This suggests that the conventional electrospray analysis denatured the protein. The LEMS measurements resulted in more folded protein ions presumably owing in part to the short interaction time (~100 ms) of the protein with the denaturing electrospray solvent and in part to nonequilibrium partitioning in the electrospray droplet (66, 73). The conformation of the lysozyme protein from an acidic electrospray solvent was probed using collision-induced dissociation; the LEMS experiment revealed no evidence for dissociation up to the highest acceleration potentials (400 V), but the conventional electrospray experiment revealed charge reduction and fragmentation at approximately 250 V, as seen in **Figure 4*c*,*d***.

To further probe the hypothesis that LEMS preserves the condensed-phase structure of the protein, measurements were performed on lysozyme in environments that allowed toggling between the folded and unfolded states (64). Controllable and reversible transitioning between partially unfolded and folded states was observed in the analysis of dehydrated and hydrated lysozyme, respectively, as shown in **Figure 5**. In this measurement, aqueous lysozyme was deposited onto a glass coverslip and interrogated to reveal the folded state (**Figure 5*a***). After the water evaporated in hot desolvation gas, lysozyme was expected to unfold, and this was observed in the LEMS measurement (**Figure 5*b***). Addition of water to the spot resulted in resolvation and refolding of the lysozyme ions (**Figure 5*c***). This series of measurements further demonstrates that LEMS is an extraordinarily soft ionization source that can reveal the condensed phase folding state of a protein. The limit of detection (LOD) for LEMS analysis of aqueous lysozyme was 17 pmol in these experiments, demonstrating sensitivity for biomolecules. This LOD is higher than those observed in protein experiments using ELDI, MALDESI, and LAESI, but it is most likely caused by the relatively low sensitivity of the mass spectrometer used for the LEMS measurements.

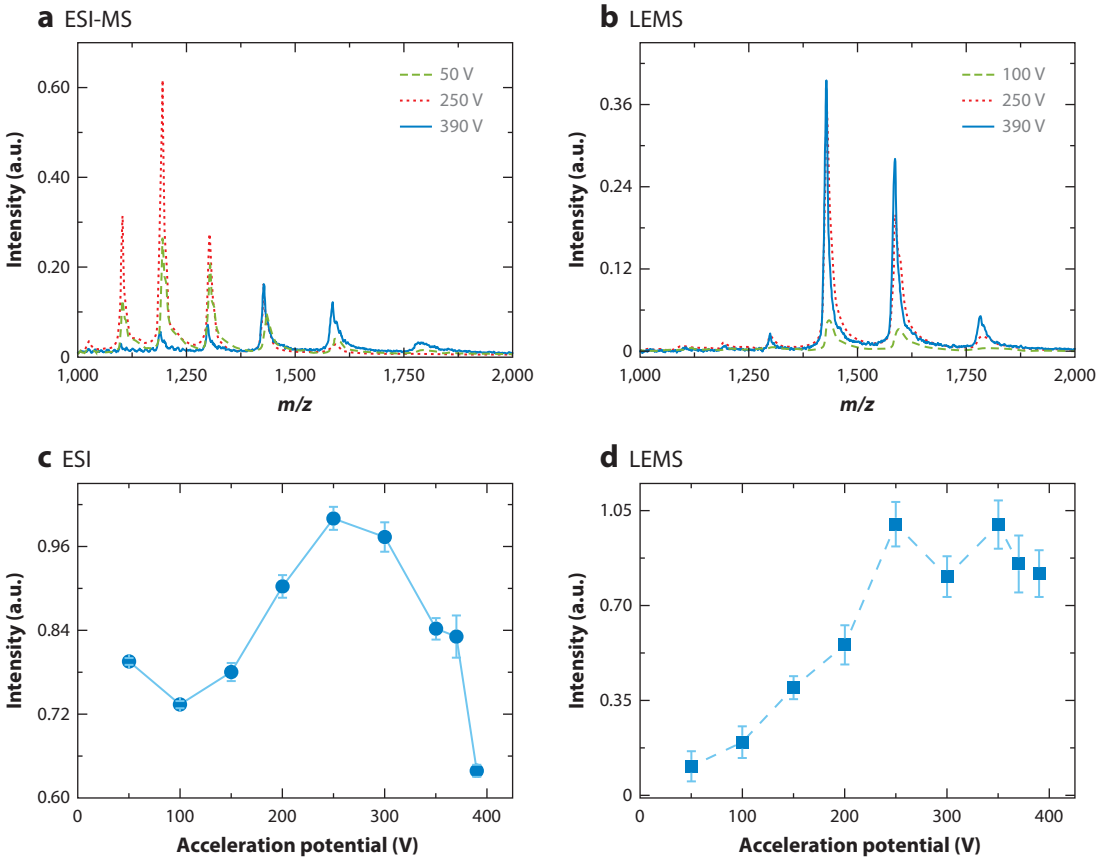

Figure 4

Mass spectra for conventional electrospray ionization mass spectrometry (ESI-MS) and laser electrospray mass spectrometry (LEMS) analysis of lysozyme at different in-source collision-induced dissociation energies are shown in panels *a* and *b*, respectively. The integrated signal intensities of lysozyme as a function of collision-induced dissociation voltage are plotted in panel *c* for ESI and in panel *d* for LEMS. In contrast to the LEMS analysis, the conventional ESI mass spectra and integrated signal intensities show charge reduction and fragmentation above 250 V. Modified with permission from Reference 65. Copyright 2011 National Academy of Sciences, USA. Abbreviations: a.u., arbitrary unit; *m/z*, mass-to-charge ratio; V, volt.

The LEMS process has several interesting properties supporting the capability for mass analysis of a wide variety of molecules, as femtosecond laser vaporization has generated gas-phase molecules regardless of the solvation and hydrophilic/hydrophobic states for subsequent electrospray ionization mass spectrometry, providing the potential for quantitative analysis of complex mixtures. Concerning robustness to the solvation state, hemoglobin from blood, albumin from hen egg white (mainly the 45-kDa protein ovalbumin), and lipids from raw egg yolk were analyzed in hydrated and dehydrated states (64) with little change in the ion intensities. In these experiments, the samples were dried for approximately 30 min in the drying gas of the Analytica of Branford electrospray source, allowing experiments on the same sample in the dry and wet states. Femtosecond vaporization was also insensitive to the degree of hydrophobicity of the sample. For instance, various types of lipids, such as fatty acids (monoolein), saturated phosphocholines with diglyceride tails [1,2-dihexanoyl-sn-glycero-3-phosphocholine (DHPC) and 1,2-dimyristoyl-sn-glycero-3-phosphocholine (DMPC)], and hydrophobic proteins (gramicidin A, B, and C), were

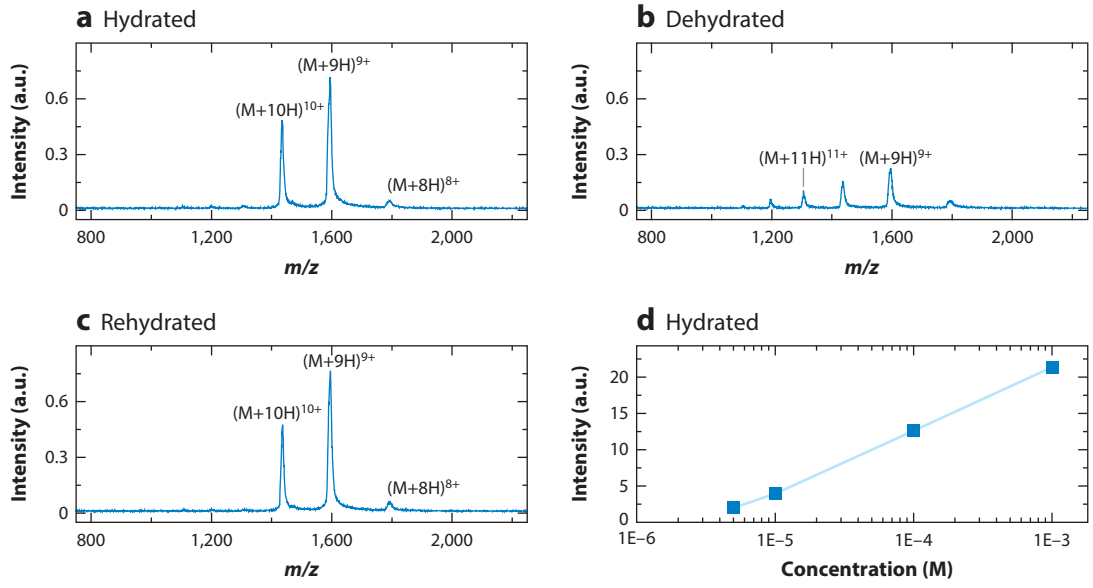

Figure 5

Laser electrospray mass spectrometry (LEMS) mass spectra of hen egg lysozyme for (*a*) hydrated, (*b*) dehydrated, and (*c*) rehydrated states, demonstrating that LEMS can determine the condensed-phase protein conformation. The mass spectral response as a function of concentration for hydrated lysozyme is shown in panel *d*. Reprinted with permission from Reference 64. Copyright 2010 American Chemical Society. Abbreviations: a.u., arbitrary unit; M, molar (mole/liter); M+H, protonated molecular ion; *m/z*, mass-to-charge ratio.

detected in experiments with LEMS using the same solvent system in the electrospray source (67). Perhaps more importantly, mixtures of monoolein and DHPC with molar ratios varying from 1:0 to 0:1 resulted in a linear relationship between the concentration of the lipid in the mixture to the measured ion intensity. The larger hydrophobic peptides, gramicidin A, B, and C, were analyzed from stainless steel and glass substrates, showing that vaporization occurs via a nonthermal mechanism. Finally, LEMS measurements of DHPC spiked into blood and measurements of lipids and proteins from dried, reduced-fat milk demonstrated that lipids in complex systems could be transferred intact into the gas phase by femtosecond vaporization (67).

Because of the nonresonant nature of the strong-field femtosecond laser vaporization process, LEMS proved capable of analyzing molecules from complex media, as was further demonstrated in the classification of plant tissue types. *Impatiens* plant petal, leaf, and stem tissues were distinguished with high accuracy (98.7%) using a compressive linear classifier after ex vivo LEMS analysis of untreated tissue samples (68). Green and white regions of the zebra plant leaf were also differentiated using the compressive linear classifier with 98.3% accuracy. However, LEMS analysis of the zebra plant resulted in fewer mass spectral features than those observed in LAESI experiments (74), most likely because LAESI ablates material from a greater depth in the z-direction, ~30–40 μm (75) in comparison with ~10 μm for LEMS. Femtosecond laser ablation depth of ~10 μm suggests that LEMS has the potential for high-resolution depth profiling. The ability of LEMS to discriminate by tissue type suggested an experiment to classify phenotypes. LEMS spectra were measured for a series of different colored *Impatiens* plant flower petals as shown in (**Figure 6**), and the application of principal component analysis (PCA) enabled highly robust discrimination of the tissue phenotype with an accuracy of 93.7% using linear discriminant analysis (LDA), which showed low root-mean-square deviations among six cross-validation sets

Figure 6

(*a*) Phenotypic discrimination of eight different *Impatiens* flower petals using laser electrospray mass spectrometry (LEMS). (*b*) The respective LEMS mass spectra, (*c*) the principal component analysis (PCA) score plot, and (*d*) the principal component analysis loadings plots are shown. The PCA score plot shows the separation among the eight groups allowing for accurate classification with linear discriminant analysis, and the PCA loading plots show the mass spectral features responsible for the separation among each principal component for the first three principal components. Modified with permission from Reference 69. Copyright 2012 American Chemical Society. Abbreviations: a.u., arbitrary unit; *m/z*, mass-to-charge ratio; PC, principal component.

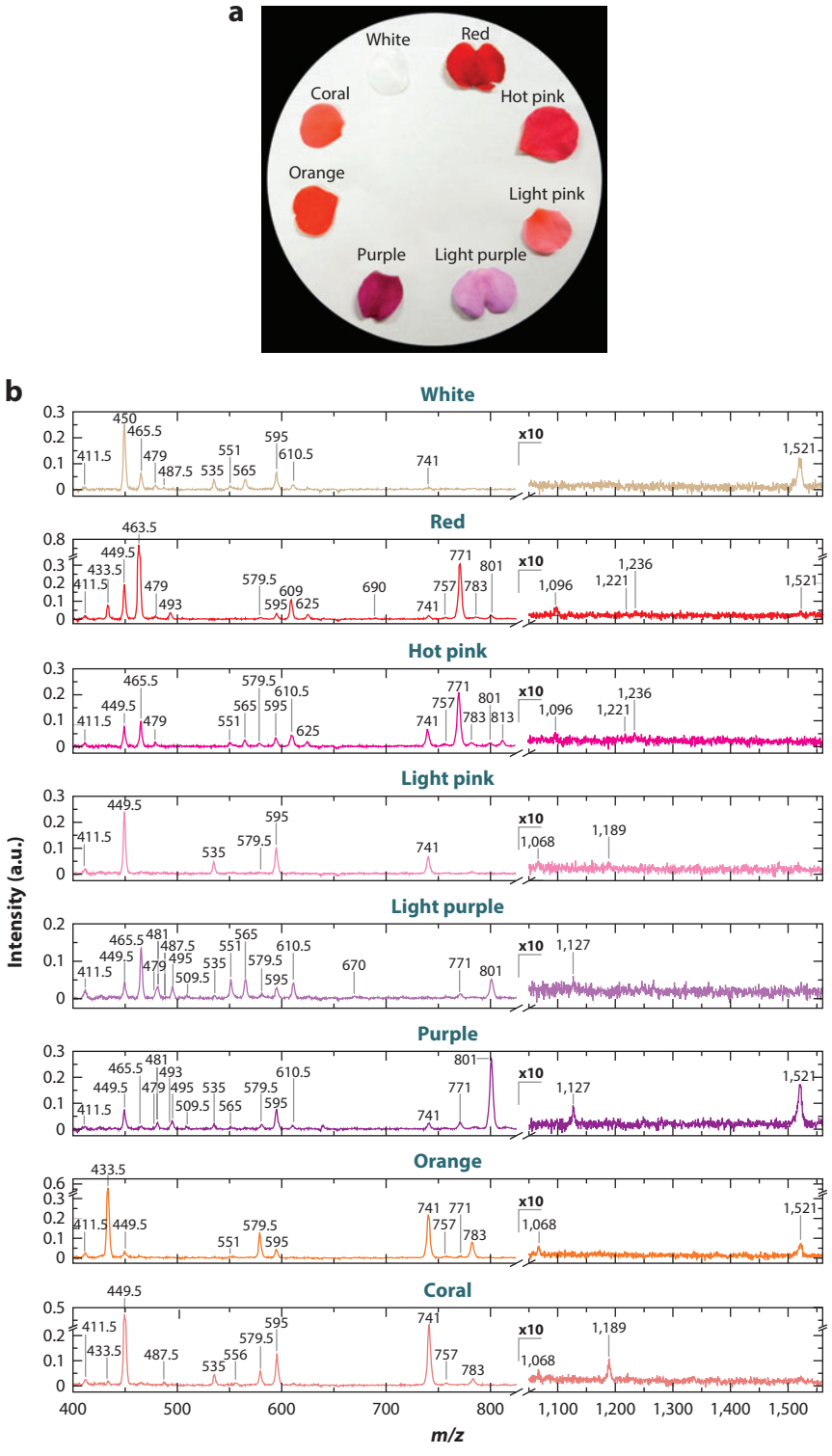

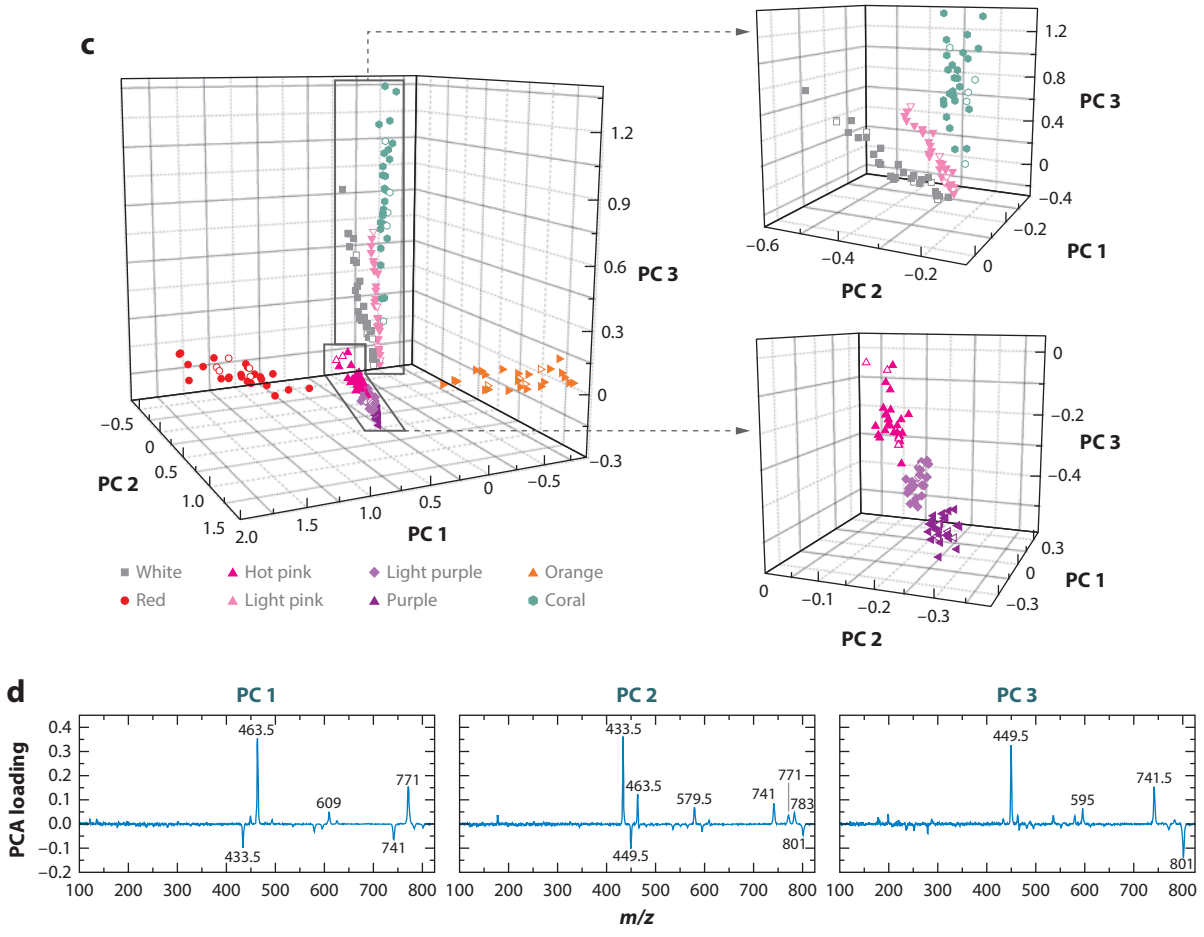

Figure 6

(*Continued*)

(69). Principal component loading values were used to locate important mass spectral features that determined the variance, which were chiefly associated with the anthocyanins that give the flower petals their colors. The measurements demonstrate the capability of LEMS, in combination with multivariate statistics, to identify biologically relevant biomarkers from complex tissue samples, similar to experiments using other ambient ionization methods.

Complex tissue analysis using LEMS is attributed to the quantitative ability of the technique in the analysis of complex mixtures. In tests of a small range of compounds, a lower degree of ion suppression was observed for multicomponent small analyte (73) and protein (66) mixtures in LEMS analyses compared to conventional ESI-MS analyses. **Figure 7** displays a comparison of the mass spectral response as a function of concentration for equimolar mixtures of three proteins using conventional ESI-MS and LEMS. As can be seen, the ESI measurements were nonquantitative because of ion suppression, whereas the LEMS measurements increased monotonically as a function of concentration providing quantitative measurements of the protein mixtures, which has been observed in a previous ESI investigation (76).

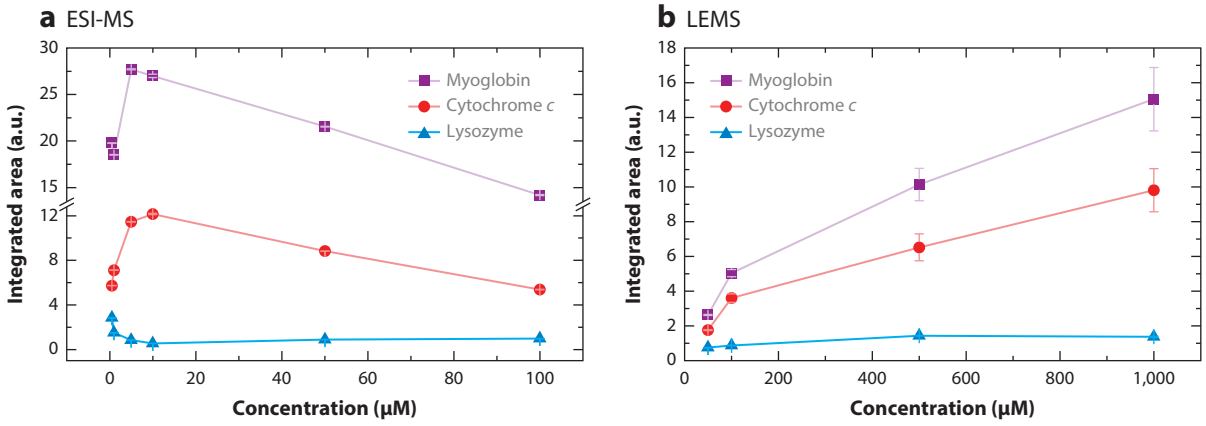

Figure 7

(*a*) Mass spectral response as a function of concentration for proteins in a three-component equimolar mixture using conventional electrospray ionization mass spectrometry and (*b*) laser electrospray mass spectrometry. Modified with permission from Reference 66. Copyright 2013 American Chemical Society. Abbreviations: a.u., arbitrary unit; ESI-MS, electrospray ionization mass spectrometry; LEMS, laser electrospray mass spectrometry.

The detection of explosives and their formulations is a new area of investigation for laser atmospheric pressure mass spectrometry, and in particular, LEMS has made considerable advances in classification of organic and inorganic explosives. The detection of dried conventional explosives, such as the nitro-containing explosive 1,3,5-trinitroperhydro-1,3,5-triazine (RDX) and taggant 2,3-dimethyl-2,3-dinitrobutane (DMNB), and the peroxide explosives 3,4,8,9,12,13-hexaoxa-1,6-diazabicyclo[4.4.4]tetradecane (HMTD) and 3,3,6,6,9,9-hexamethyl-1,2,4,5,7,8-hexaoxacyclononane (TATP) from stainless steel substrates was achieved using LEMS with nanogram sensitivity (77). A pellet of a complex RDX formula containing plasticizers and binders was also successfully analyzed, resulting in features for RDX and ethyl centralite, the main stabilizer in the propellant formulation. Vaporization using 400-μJ laser pulses focused to 250 μm in diameter, followed by postionization using an electrospray solvent including NaCl and KCl to give sodiated- and potassiated-adduct features, largely resulted in the transfer of the explosives into the gas phase without fragmentation except for the highly unstable peroxide explosives. RDX was detected from sand with remote detection 2 m away from the mass spectrometer inlet, demonstrating explosive detection from complex and realistic substrates (78). In this experiment, a Venturi air jet pump enabled transfer of the RDX molecules through polyethylene tubing from the vaporization spot to the electrospray plume for ionization and mass analysis.

Other types of explosives, such as inorganic-based explosives (78, 79) and smokeless powders (80), have been analyzed using LEMS and classified using multivariate statistics. In the case of inorganic explosives, a number of positive and negative ions, as well as neutrals, must be detected regardless of charge state to enable classification. Tailoring the electrospray solvent for inorganic explosives included analyzing cationic pairing agents, the lipid monoolein, and sodium acetate to enable the simultaneous detection of cationic, anionic, and neutral signature features from four different inorganic-based explosive compositions. Classification of the four simulated inorganic improvised explosive device (IED) signatures resulted in 99% accuracy using LDA after PCA was performed on a library of 40 signature features. The LEMS mass spectra for the four inorganic IEDs and the PCA score plot are shown in **Figure 8**. The LOD with LEMS was determined to be approximately two orders of magnitude higher than conventional ESI-MS in the complexation

analysis of ammonium nitrate (79) due to ~1% capture and ionization efficiency. The detection and classification of an unknown five-component system, including chlorate-perchlorate sugar, ammonium nitrate, the RDX propellant formulation, and preblast and postblast firework residue, were also enabled with the same methodology, including the electrospray complexation mixture and multivariate statistics (78). An investigation of five smokeless powders was performed using LEMS (80). Analysis of the powders after removal from their cartridges (two rifle and three pistol cartridges) resulted in the detection of many organic stabilizers and plasticizers commonly found in smokeless powders, as well as new compounds that have not been previously reported in the manufacturers' specifications. Classification using PCA and LDA resulted in 100% accuracy and principal component loading values revealed the important mass spectral features for classification, as shown in **Figure 9**.

Electrospray-Assisted Laser Desorption/Ionization

Atmospheric pressure laser desorption in combination with electrospray ionization mass spectrometry was first reported in 2005 (81). The ELDI technique used a nitrogen laser with a wavelength of 337 nm and pulse duration of 4 ns to desorb a variety of molecules from surfaces into the gas phase for subsequent ESI mass spectral analysis. Measurements of dried cytochrome *c* from a stainless steel surface with or without a MALDI matrix revealed a charge-state distribution corresponding to unfolded cytochrome *c*. One could speculate that the red colored protein served as the matrix, absorbing the 337-nm photon, but a subsequent paper demonstrated the ability to detect dried lysozyme and myoglobin, as well as other proteins in biological media, i.e., from bacterial cultures, and porcine liver and heart tissue samples (82). Although the mechanism of vaporization has not yet been elucidated, the substrate likely plays a role in the desorption event. Analysis of basic blue 7 from a stainless steel substrate produced the best signal intensity compared to other substrates, presumably due to thermal effects (83). Ionization was proposed (82, 84) to occur through modified fused-droplet electrospray ionization (85–87), where laser-desorbed analytes are ionized through fusion with charged solvent droplets. This hypothesis was supported by the observation of ESI-like, multiply charged protein ions. ELDI also enabled surface analysis of other dried samples including major components in milk, colors of a painting, coating of a compact disc, drug tablets, porcine brain tissue (84), and inks (88). Imaging with a resolution of 250 μm was demonstrated using ELDI on fungal and animal tissue samples (36, 89). ELDI has been used in two-dimensional (2D) analyses for detection of compounds after thin-layer chromatography (TLC) separation with either pulsed UV (90, 91) or IR laser beams (91).

To enable the desorption of folded protein from liquid samples, carbon powder was added to the sample solutions, absorbing the laser energy in a manner similar to Tanaka's cobalt powder (9) and enabling the transfer of native folded protein into the gas phase for mass analysis (92). Liquid ELDI measurements with MALDI matrices, which increased the ion signal in comparison with matrix-free analysis, led to protein unfolding (93). A four-component protein mixture was quantified with ELDI, whereas neither MALDI nor ESI measurements reflected the protein concentration owing to ion suppression (92). ELDI has been used to monitor reactions by suspending carbon powder in liquid sample solutions to enable laser desorption (94). Reactive ELDI experiments that occur from the fusion of reactants into the electrospray droplets have been performed with the reactant in the electrospray solvent and the analyte being desorbed from a sample surface, or vice versa (95).

The desorption yield was measured as a function of laser wavelength and fluence for cytochrome *c* at 337 nm from a nitrogen laser and at 266, 532, and 1,064 nm from a Nd:YAG laser (83). The highest cytochrome *c* ion intensity occurred when using laser pulses with 1,064-nm light for liquid samples without an added matrix, presumably owing to the proximity of the resonant OH bending

vibrations of water molecules at 1,050 nm. More background ions were produced in analyses using organic matrices or desorption with UV laser light at 266 nm. The use of an IR optical parametric oscillator laser with ESI postionization, termed IR-ELDI, allowed the optimization of large biomolecule mass analysis after desorption without a matrix by nanosecond laser pulses centered at 2.74 or 2.94 μm with pulse energies of 150 μJ (96). Sensitivity was greatly increased

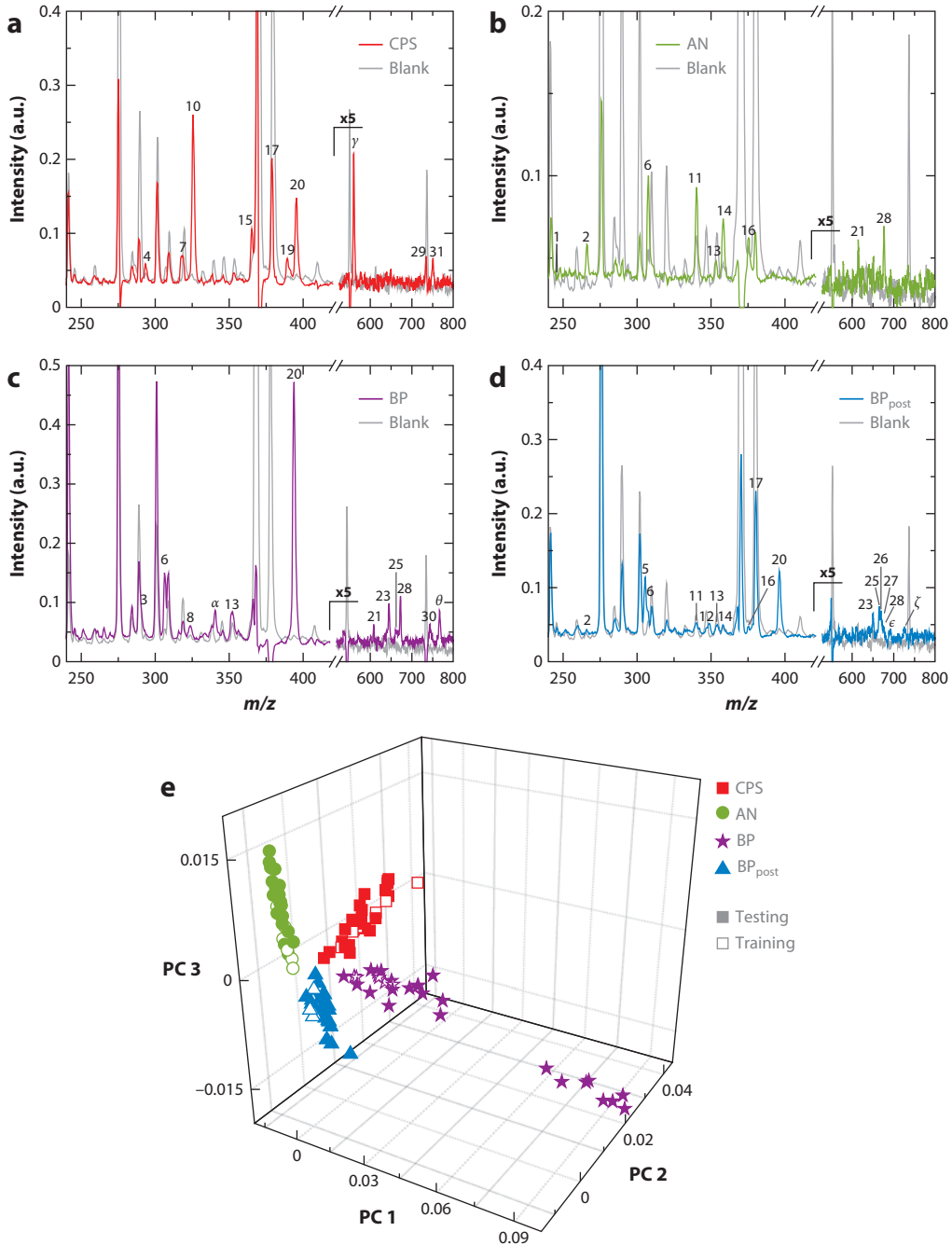

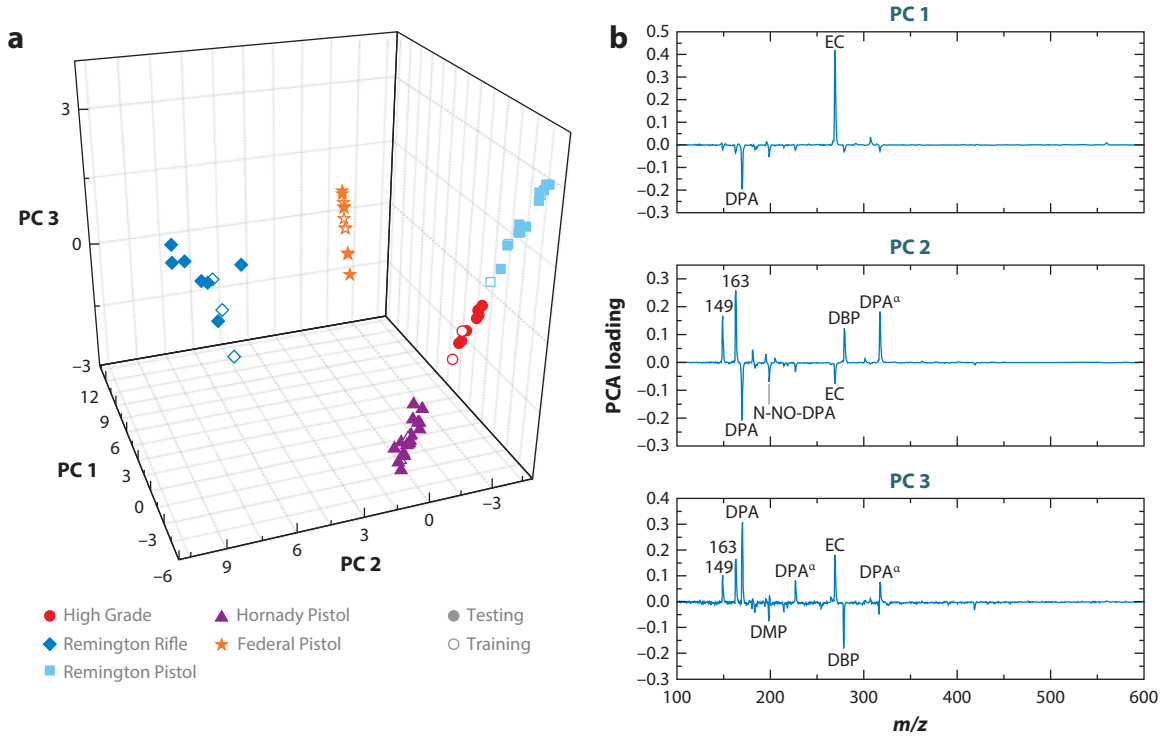

Figure 9

(*a*) Principal component analysis (PCA) of five different commercially available smokeless powders projected into three dimensions for high grade (*red* ●), Remington rifle (*blue* ◆), Remington pistol (*cyan* ■), Hornady pistol (*purple* ▲), and Federal pistol (orange ★). This analysis shows the separation between manufactures' powders. The open symbols (○, ◇, □, △, and ☆) and the filled colored symbols (●, ◆, ■, ▲, and ★) represent the training and testing sets for each smokeless powder, respectively. (*b*) PCA loading plots for the first three principal components (PCs) from the LEMS analysis of five different smokeless powders. These plots show important mass spectral features that are used to discriminate each ammunition. Modified with permission from Reference 80. Copyright 2013 American Chemical Society. Abbreviations: DBP, dibutyl phthalate; DMP, dimethyl phthalate; DPA, diphenylamine; EC, ethyl centralite; N-NO-DPA, N-nitrosodiphenylamine; *m/z*, mass-to-charge ratio.

in the analysis of sample solutions with a two orders of magnitude sensitivity gain compared with UV-ELDI for peptide analysis as water acts as a matrix with mid-IR laser pulses, similar to LAESI (97) and IR-matrix-assisted laser desorption electrospray ionization (IR-MALDESI) (98) experiments. The limits of detection for bradykinin, ubiquitin, and carbonic anhydrase were lowered to 250, 100, and 500 femtomole (fmol), respectively, using IR-ELDI.

←

Figure 8

Laser electrospray mass spectrometry (LEMS) spectra (ESI background subtracted, with the ESI background spectra in *gray*) showing characteristic peaks for four inorganic explosive materials: (*a*) chlorate, perchlorate, and sugar; (*b*) ammonium nitrate; (*c*) preblast black powder; and (*d*) simulated, postblast black powder. (*e*) Principal component analysis (PCA) projected into three dimensions for chlorate, perchlorate, and sugar (*red* ■), ammonium nitrate (*green* ●), preblast black powder (*purple* ★), and postblast black powder (*blue* ▲) simulated improvised explosive devices (IEDs) show separation among the four inorganic-based IEDs. The open symbols (□, ○, ☆, and △) and the filled, colored symbols (■, ●, ★ , and ▲) represent the training and testing sets for each IED, respectively. Modified with permission from Reference 79. Copyright 2011 American Chemical Society. Abbreviations: a.u., arbitrary unit; *m/z*, mass-to-charge ratio.

Matrix-Assisted Laser Desorption Electrospray Ionization

Although ELDI demonstrated the ability to desorb samples with nanosecond UV laser pulses without a matrix, subsequent experiments reported that an organic matrix significantly improved the desorption of analytes using a nitrogen laser (70). In the first report, various protein and peptide samples were dissolved in a sinapinic acid matrix, desorbed from stainless steel substrates using 4-ns, 120-μJ laser pulses centered at 337 nm and ionized using nano-ESI. The multiple charging of proteins BNP-32 and ubiquitin observed in the MALDESI experiment with a remote analyte sample, transport, and ionization relay (RASTIR) setup validated the ionization mechanism as electrospray postionization and not MALDI ionization (99). Remote desorption of reserpine transported by the RASTIR device to an electrospray plume containing deuterated solvents revealed that the $[M+D]^+$ features were abundant even though reserpine does not undergo significant hydrogen/deuterium (H/D) exchange (100). Some $[M+H]^+$ ions were observed, most likely due to AP-MALDI processes. Remote sampling alleviated the problems of interfering MALDI target plate and ESI emitter voltages and low ionization efficiency with MALDESI, which was improved to 1.5% with the RASTIR source (101).

Like ELDI, MALDESI was also used to analyze liquid samples of peptides and proteins (1 to 8.6 kDa) contained by an organic matrix (102). Ionization of the desorbed droplets still occurred without ESI postionization when the sample target was biased to higher voltages (normally at 500 V; increased to 3 kV) with the desorbed droplet acting as the electrospray droplet. Multiple charging of peptides and proteins without ESI postionization was previously reported in the vaporization of dehydrated sample droplets containing glycerol using AP-IR-MALDI (103).

MALDESI was performed on solid and liquid samples using 7-ns IR laser pulses centered at 2.94 μm (98), and these IR-MALDESI analyses of solid-state samples using organic matrices revealed mass spectral responses similar to experiments with UV laser pulses. For instance, top-down protein characterization was performed on solid protein samples using organic matrices and either UV (104) or IR laser pulses (98). In the work comparing UV- and IR-MALDESI mass spectra of bovine milk and egg yolk, more features were revealed with IR-MALDESI because water molecules act as a matrix for 2.94-μm light, similar to LAESI (97) and IR-ELDI (96). IR-MALDESI was also used to analyze proteins and O-linked glycans cleaved from mucin (98) as well as dyes from fabric textiles (105).

Analysis with IR laser pulses focused to 250 μm in diameter provided spatially resolved images down to 45 μm using an oversampling technique for rat brain, mouse heart, and lung tissue samples (106). Internal mass calibration with ambient polydimethylcyclosiloxane ions allowed accurate measurement of the frequency shift of a Fourier transform ion cyclotron resonance mass spectrometer, enabling a resolving power of 100,000 full width at half maximum (FWHM) at 400 *m/z* (107). In an imaging analysis of mouse brain tissue, lipids that were previously convoluted could be baseline separated in the mass spectra, leading to better spatially resolved images of the mouse brain for the two lipids.

Although low neutral capture efficiencies of less than 0.02% were common in the infancy of MALDESI (70), the sensitivity was subsequently greatly increased by the optimization of parameters. Using a stable isotope-labeled analog as a calibrant in the electrospray, the LOD was determined to be 630 attomole (amol) for the polypeptide angiotensin I (104). The LOD for IR-MALDESI was reduced four orders of magnitude from 100 fmol to 10 amol for cytochrome *c* through the systematic optimization of parameters, called the design of experiments (71). The key experimental parameters included flow rate (nanospray > electrospray), sample-inlet distance (vaporization closer to the ESI emitter is best), and laser fluence (best around 1.5 mJ).

Laser Ablation Electrospray Ionization

IR lasers have become more commonplace in mass spectral analysis because many matrices absorb IR light (23), including water where the OH stretch is ~2.9 μm. Use of water as a matrix allows reduced sample preparation, particularly for the analysis of biological samples at atmospheric pressure as was first demonstrated in AP-IR-MALDI studies (108). Mid-IR absorption leads to higher desorption yields in comparison with UV excitation because of a higher IR penetration depth (37, 109–110). Laser desorption using nanosecond, mid-IR laser pulses at atmospheric pressure consists of a two-stage process (111–113) that results in the plume being composed of particles (114, 115) and molecules (116) with low ionization yields (24). The increased production of neutral molecules (110) leads to lower sensitivities than UV-MALDI experiments with conventional MALDI matrices (108). To increase ion signals from mid-IR laser vaporization at atmospheric pressure, IR laser desorption was coupled with electrospray for postionization and called LAESI (97, 117). Imaging studies revealed that LAESI yielded higher ion intensities by one or two orders of magnitude than AP-IR-MALDI (24) because of the postionization process. LAESI uses <100-ns (often 7-ns), 2.94-μm laser pulses at a 90° incidence angle for ablation of any water containing sample into the gas phase for subsequent ionization by an electrospray source. LAESI produces internal energy distributions comparable to conventional electrospray as observed in the analysis of para-substituted benzylpyridinium ions in solid or condensed phases (118). Analysis of peptides and vitamin B_{12} using LAESI and ESI showed no fragmentation, contrary to the fragments observed with vacuum UV-MALDI. In the initial LAESI analysis, the technique enabled the detection of a variety of molecules up to 66 kDa with a spatial resolution of ~400 μm for proteins, lipids, and metabolites, including analytes from whole blood, serum, and different plant tissues (97). Using flash shadowography, the vaporized plume was shown to interact with the electrospray droplets, giving credence to the fused-droplet theory proposed by Shiea & Wang (87).

Imaging experiments have been performed on tissue samples due to excitation of the water in biological samples by the laser pulses used in LAESI. Two-dimensional imaging of zebra plant leaves, using 2-mJ pulses focused to a lateral resolution of ~350 μm, resulted in the mass spectral and spatial identification of metabolites responsible for the green and yellow colors of the leaf and detection of various other metabolites in depth profiling analyses (74). Depth profiling combined with 2D imaging yielded 3D images of zebra plant and peace lily leaves with increased lateral and depth resolutions of ~300 and 30–40 μm, respectively (75). Tandem mass spectrometry led to accurate metabolite identification, and with their locations found by using 3D imaging, correlations of the metabolic biochemical roles in the plant were discovered. Two-dimensional imaging with a smaller spot size and a lower pulse energy was performed for metabolites and lipids from rat brain tissue (119). A Peltier cooling stage was incorporated in the LAESI setup to prevent dehydration of the brain tissue as required by the analysis time of ~3 hours. Pearson colocalization maps, utilized previously in a 3D imaging study of the plant tissues (75), revealed biological correlations between lipids and smaller metabolites.

LAESI experiments have focused on higher spatial resolution mass spectral analysis of cells (120–122). Using an etched tip of a GeO_2-based glass fiber, mid-IR laser pulses were focused to spot sizes of 30–40 μm for in situ metabolic profiling of onion and daffodil bulb epidermals of ~20–200 μm in diameter as well as sea urchin egg cells of ~100 μm in diameter (120). The cell walls of turgid cells were ruptured by the second laser pulse from the glass fiber, enabling ablation of the cytoplasm. Disparities in the metabolite ion signals were discovered in cells of the same type but from different species (onion versus daffodil bulb), colorless and pigmented (purple) onion cells, and cells of different ages (from different layers of the onion bulbs). LAESI-MS signals taken from single cells diminished after ~50 s or 100 laser pulses because evaporative drying competes with cytoplasm

ejection from laser ablation (121). In situ cell-by-cell imaging of onion epidermal cells, oil glands from sour orange leaf cells, and human buccal epithelial (cheek) cells has also been performed (122). A multivariate statistical analysis tool, orthogonal projections to latent structures discriminant analysis, performed on the obtained LAESI mass spectra distinguished the variance between different cell types and revealed the metabolites responsible for the variance. An overview of in vivo and in situ biological tissue and cell imaging using ambient mass spectral techniques was reported (37).

LAESI experiments using ~300-μm diameter desorption pulses were also performed for metabolic profiling of whole-cell populations (123, 124) and cyanobacteria (125). LAESI mass spectra were used to discover changes in metabolites and lipids for human T-lymphotropic virus type 1- and type 3-transformed cells and for Tax1- and Tax3-expressing cell lines (123). LAESI-MS and orthogonal projections to latent structures discriminant analysis were employed to investigate viral takeover of cell populations in oncovirus-infected B-lymphocytes (124). Further LAESI metabolic profiling experiments were performed on intact cyanobacteria, revealing the ratio of phycocyanin and allophycocyanin proteins in the antenna complex, the subunit composition of phycobiliproteins, and the identity of 30 metabolites and lipids (125).

Mid-IR ablation of a liquid sample using an etched optical fiber located within a capillary was used to confine the radial expansion of the ablated plume (126), resulting in a reduction of the LOD by an order of magnitude to 600 amol for verapamil and an extension of the dynamic range to six decades in comparison to conventional LAESI (97) with a LOD of 8 fmol and a dynamic range of four orders of magnitude. Heat-assisted laser ablation electrospray ionization mass spectrometry (127) combined the ionization techniques from conventional LAESI with laser ablation atmospheric pressure photoionization (LAAPPI) (128) and enabled simultaneous detection of polar and nonpolar analytes, perhaps owing to secondary electrospray ionization (129). Because gas phase proton affinities are typically higher than those in the liquid phase, ionization of less polar compounds can then occur.

Several techniques similar to LAESI have been developed. Infrared laser-assisted desorption electrospray mass spectrometry (IR-LADESI), using an Er:YAG laser at 2.94 μm with a temporal pulse width of 100 ns, enabled detection of aqueous cytochrome *c* and bradykinin, and untreated human whole blood and urine samples (130). Later measurements with IR-LADESI were coupled with an atmospheric pressure drift tube ion mobility spectrometer to screen for the active pharmaceutical ingredients in antimalarial tablets to identify counterfeit drugs (131). Infrared laser desorption electrospray ionization (IR-LDESI), using a 10.6-μm CO_2 laser with a pulse energy of <100 μJ at 5kHz repetition rate, was employed for ablation of condensed-phase proteins of molecular masses from 8.6 to 17 kDa and electrospray postionization mass spectrometry (132). Laser ablation mass spectrometry (LAMS), employing a tunable IR laser for 5 ns and 2.94-μm pulses with pulse energies of 2 mJ, was utilized in the characterization of analyte surface activity and solute partitioning between bulk-liquid and the liquid-gas interface in droplets (133). Chemical fingerprinting of dairy products and classification using PCA were performed on mass spectra obtained with a technique termed laser desorption spray postionization (LDSPI), which used a pulsed 10-ns, 1,064-nm Nd:YAG laser with a pulse energy of 11 mJ to desorb liquid analytes into an electrospray source for postionization (134). In a subsequent experiment, analysis of insulin from stainless steel or copper substrates led to iron-insulin and copper-insulin complexes, indicating ablation of the substrate by the 1.1-mJ laser pulses (135). In a novel LDSPI experiment, two electrospray needles were used for selective ionization of desorbed samples, enabling selective detection of food components and manipulation of protein charge-state distributions (136). By quickly switching the voltages to the two electrospray emitters, desorbed analytes could interact with different solvents and reagents.

OTHER TWO-STEP METHODS

Laser Ablation Sample Transfer for Electrospray Ionization Analysis

Laser ablation of a sample into a droplet suspended above the sample surface has been investigated as a means for introduction to an ESI system. Dye molecules have been ablated with a 532-nm laser (5-μJ pulse energy) into a hanging droplet positioned above the sample surface using a commercially available autosampler syringe injection needle for direct infusion ESI-MS or for ESI-MS after high-performance liquid chromatography separation (137). Imaging of dye molecules with 100-μm resolution was demonstrated using ablation in transmission geometry by an 11-ns, 337-nm N_2 laser into a continuous flow ESI probe, termed the liquid microjunction surface sample probe (138). A 5-ns IR-pulsed laser centered at 2.94 μm has been employed for the ablation of proteins into a hanging liquid droplet from a syringe for either deposition on a MALDI target for offline MALDI analysis or for flow-injection into a nano-ESI source (139). IR ablation in transmission geometry enabled the online separation of peptide and protein mixtures using high-performance liquid chromatography (140) and capillary electrophoresis (141) for subsequent ESI mass analysis. Collection of laser-ablated materials was enhanced two orders of magnitude by applying a voltage of ~1 kV directly to a hanging droplet or to a flowing liquid bridge for subsequent ESI analysis (142).

Laser-Based Acoustic Desorption

Laser pulses have enabled mass spectral analysis through acoustic desorption of analytes followed by a separate postionization event. Typically in laser-induced acoustic desorption (LIAD) methods, highly energetic laser pulses irradiate the opposite side of a metal foil on which the sample has been deposited, causing analytes to be desorbed into the gas phase by the resulting shock wave. LIAD using a 1,064-nm laser with a pulse duration of 9 ns and pulse energies of 20 to 30 mJ followed by ESI postionization enabled the mass spectral analysis of amino acids, peptides, and proteins from the solid-state and solution phases (143). LIAD-ESI was later utilized in the analysis of separated molecules from thin-layer chromatography plates, although glycerol had to be sandwiched between a glass plate and the aluminum-backed thin-layer chromatography plate to enable LIAD (144).

SINGLE-STEP PROCESSES: DESORPTION AND IONIZATION

Although most atmospheric pressure laser ablation/desorption techniques utilize postionization methods because of the low direct ionization yield, there are single-step ambient techniques that use laser pulses for desorption and ionization. The laserspray ionization inlet technique (LSII) (26, 27, 145) is similar to AP-MALDI but produces ESI-like multiply charged ions. The term laserspray ionization (LSI) encompasses experiments performed under AP conditions (LSII) as well as those performed at intermediate pressure (146, 147) and under vacuum conditions (148), designated laserspray ionization vacuum. Multiply charged protein ions with charge-state distributions were first noted in AP-IR-MALDI analyses of proteins from a glycerol matrix (103). Typically in LSI experiments, sample molecules from a matrix are ablated at atmospheric pressure with a UV nanosecond laser centered at 337 or 355 nm. The molecules are ablated in transmission geometry in a field-free region and are then transferred into the vacuum of the mass spectrometer by a heated ion transfer capillary. Ablation of a sample in the transmission geometry allows the sample to be closer to the mass spectrometer inlet, enhancing the sensitivity of AP-MALDI as the expanding

sample plume diffuses directly into the vacuum (26). LSI has also been performed by laser ablation in reflection geometry (149). Multiply charged ions are generated from molten matrix clusters, resulting from the laser desorption process, which are desolvated and declustered in the heated transfer region (150). The observed charge states depend on the matrix, the energy imparted to produce droplets/clusters, the size of the clusters produced, and the available desolvation time. Higher laser powers and voltages increase the abundance of singly charged ions (151). Multiply charged ions were observed under field-free laser vaporization phase conditions, whereas applying a potential to the sample plate (~1 kV) resulted in singly charged protein ions typically observed in AP-MALDI experiments (149). LSII has been used with ion mobility spectrometry for the solvent-free gas-phase separation and mass analysis of proteins (152), isomeric β-amyloid compounds (153), and peptide and lipids from mouse brain (147). Further LSII analysis of mouse brain tissue resulted in the imaging of lipids with a spatial resolution of 20 μm (154) and protein characterization from delipified mouse brain tissue using electron transfer dissociation (155). A one-step method that produced multiply charged ions from laser desorption and ionization, similar to LSII and experiments with MALDESI (102) and IR-LDESI (132) without ESI postionization, was high-voltage-assisted laser desorption ionization (HALDI) (156). Liquid samples without an organic matrix deposited on a sample target biased to high voltage (~5 kV) were desorbed and ionized by 10-ns, 1,064-nm laser pulses with a pulse energy of ~1 mJ or higher. In this way, multiply charged ions (in positive and negative modes) were detected for proteins, oligonucleotides, drugs, milk, and chicken eggs.

Various types of lasers and wavelengths have been used in one-step laser desorption and ionization mass spectral methods. In one study, two different lasers, a 10.6-μm surgical CO_2 laser with a pulse duration of 90 μs and pulse energies of 10 to 30 mJ and a 355-nm Nd:YAG laser with a pulse width of 4 ns and energy of 8 mJ, were utilized in the mass spectral analysis of healthy and diseased tissue samples (157). No mass spectra were obtained using visible or near-IR nanosecond laser pulses, which is why most atmospheric pressure laser ablation methods utilize postionization. The ablated and ionized tissue molecules, mostly phospholipids, were transferred to the mass spectrometer by a Venturi pump. Differentiation of various tissue types and diseased states were accomplished by PCA. In a LSI-like experiment, a 45-fs, 800-nm laser pulse with energy of 3 to 15 μJ enabled mass spectral analysis of dyes and a monolayer of onion epidermis (158). This method was named atmospheric pressure femtosecond laser desorption ionization imaging mass spectrometry (AP-fs-LDI-IMS) and enabled the imaging of the onion epidermis with a spatial resolution of ~10 μm. Unlike LEMS (43), no postionization process was employed, as interaction with the intense laser pulses (10^{14} W cm^{-2}) enabled ablation, fragmentation, and ionization of the small molecules.

SUMMARY POINTS

1. Femtosecond laser pulses couple energy directly into analytes via nonresonant, multiphoton excitation on an ultrafast timescale. Using 800-nm, 70-fs duration pulses at 10^{13} W cm^{-2} enables release of analytes into the gas phase for all systems studied to date.
2. Femtosecond laser vaporization, in combination with electrospray ionization and time-of-flight mass spectrometry, results in a rapid analysis system that is capable of probing van der Waals–bonded, condensed-phase systems. This method is called laser electrospray mass spectrometry (LEMS).

3. To date, pharmaceuticals, explosives, narcotics, lipids, and proteins have been analyzed quantitatively and in multicomponent mixtures without the limitations of charge suppression and saturation that are present in conventional ESI-MS analysis.
4. Femtosecond laser vaporization has been shown to preserve the condensed-phase structures of protein molecules from native and denaturing conditions as measured through the resulting mass spectral charge-state distributions. This allows the rapid determination of their solid-state or solution protein structures.
5. LEMS has been used to classify the type of formulation for organic and inorganic classes of explosives. In the case of inorganic explosives, a mixture of complexation agents allowed the determination of cations, anions, and neutrals using a single electrospray solvent system. In the case of smokeless powders, five different manufacturers were classified with 100% accuracy.
6. LEMS has been used to classify plant organ types as well as phenotypes as demonstrated by the accurate determination of flower petal color for eight different flower colors from the same species.
7. LEMS is suitable for spatially resolved analysis with a resolution of 75 μm.

DISCLOSURE STATEMENT

The authors are not aware of any affiliations, memberships, funding, or financial holdings that might be perceived as affecting the objectivity of this review.

ACKNOWLEDGMENTS

We gratefully acknowledge the support of the National Science Foundation through awards CHE0518497 and CHE0957694 and the support of the Office of Naval Research through award N00014-10-0293.

LITERATURE CITED

1. Maiman TH. 1960. Stimulated optical radiation in ruby. *Nature* 187:493–94
2. Zandee L, Bernstein RB. 1979. Laser ionization mass spectrometry: extensive fragmentation via resonance-enhanced multiphoton ionization of a molecular benzene beam. *J. Chem. Phys.* 70:2574–75
3. Hillenkamp F, Unsöld E, Kaufmann R, Nitsche R. 1975. Laser microprobe mass analysis of organic materials. *Nature* 256:119–20
4. Barber M, Bordoli RS, Sedgwick RD, Tyler AN. 1981. Fast atom bombardment of solids (FAB): A new ion source for mass spectrometry. *J. Chem. Soc. Chem. Commun.* 293:325–27
5. Benninghoven A, Rudenauer F, Werner HW. 1987. *Secondary Ion Mass Spectrometry: Basic Concepts, Instrumental Aspects, Applications and Trends*. New York: Wiley
6. Sundqvist B, Macfarlane RD. 1985. ^{252}Cf-plasma desorption mass spectrometry. *Mass Spectrom. Rev.* 4:421–60
7. Yamashita M, Fenn JB. 1984. Electrospray ion source. Another variation on the free-jet theme. *J. Phys. Chem.* 88:4451–59
8. Yamashita M, Fenn JB. 1984. Negative ion production with the electrospray ion source. *J. Phys. Chem.* 88:4611–15
9. Tanaka K, Waki H, Ido Y, Akita S, Yoshida Y, et al. 1988. Protein and polymer analyses up to *m/z* 100,000 by laser ionization time-of-flight mass spectrometry. *Rapid Commun. Mass Spectrom.* 2:151–53

10. Karas M, Bachmann D, Bahr U, Hillenkamp F. 1987. Matrix-assisted ultraviolet laser desorption of non-volatile compounds. *Int. J. Mass Spectrom. Ion Process.* 78:53–68
11. Karas M, Hillenkamp F. 1988. Laser desorption ionization of proteins with molecular masses exceeding 10,000 daltons. *Anal. Chem.* 60:2299–301
12. Hillenkamp F, Karas M, Beavis RC, Chait BT. 1991. Matrix-assisted laser desorption/ionization mass spectrometry of biopolymers. *Anal. Chem.* 63:1193–203
13. Takats Z, Wiseman JM, Gologan B, Cooks RG. 2004. Mass spectrometry sampling under ambient conditions with desorption electrospray ionization. *Science* 306:471–73
14. Wolfender JL, Chu F, Ball H, Wolfender F, Fainzilber M, et al. 1999. Identification of tyrosine sulfation in *Conus pennaceus* conotoxins α-PnIA and α-PnIB: further investigation of labile sulfo- and phosphopeptides by electrospray, matrix-assisted laser desorption/ionization (MALDI) and atmospheric pressure MALDI mass spectrometry. *J. Mass Spectrom.* 34:447–54
15. Laiko VV, Baldwin MA, Burlingame AL. 2000. Atmospheric pressure matrix-assisted laser desorption/ionization mass spectrometry. *Anal. Chem.* 72:652–57
16. Gabelica V, Schulz E, Karas M. 2004. Internal energy build-up in matrix-assisted laser desorption/ionization. *J. Mass Spectrom.* 39:579–93
17. Moyer SC, Cotter RJ. 2002. Peer reviewed: Atmospheric pressure MALDI. *Anal. Chem.* 74:468a–76a
18. Creaser CS, Ratcliffe L. 2006. Atmospheric pressure matrix-assisted laser desorption/ionisation mass spectrometry: A review. *Curr. Anal. Chem.* 2:9–15
19. Koestler M, Kirsch D, Hester A, Leisner A, Guenther S, Spengler B. 2008. A high-resolution scanning microprobe matrix-assisted laser desorption/ionization ion source for imaging analysis on an ion trap/Fourier transform ion cyclotron resonance mass spectrometer. *Rapid Commun. Mass Spectrom.* 22:3275–85
20. Guenther S, Römpp A, Kummer W, Spengler B. 2011. AP-MALDI imaging of neuropeptides in mouse pituitary gland with 5 μm spatial resolution and high mass accuracy. *Int. J. Mass Spectrom.* 305:228–37
21. Harada T, Yuba-Kubo A, Sugiura Y, Zaima N, Hayasaka T, et al. 2009. Visualization of volatile substances in different organelles with an atmospheric-pressure mass microscope. *Anal. Chem.* 81:9153–57
22. Li Y, Shrestha B, Vertes A. 2007. Atmospheric pressure molecular imaging by infrared MALDI mass spectrometry. *Anal. Chem.* 79:523–32
23. Li Y, Shrestha B, Vertes A. 2008. Atmospheric pressure infrared MALDI imaging mass spectrometry for plant metabolomics. *Anal. Chem.* 80:407–20
24. Vertes A, Nemes P, Shrestha B, Barton AA, Chen Z, Li Y. 2008. Molecular imaging by mid-IR laser ablation mass spectrometry. *Appl. Phys. A* 93:885–91
25. Sheehan EW, Willoughby RC. 2006. Ion enrichment aperture arrays. *US Patent No. 7,060,976*
26. Trimpin S, Herath TN, Inutan ED, Cernat SA, Miller JB, et al. 2009. Field-free transmission geometry atmospheric pressure matrix-assisted laser desorption/ionization for rapid analysis of unadulterated tissue samples. *Rapid Commun. Mass Spectrom.* 23:3023–27
27. Trimpin S, Inutan ED, Herath TN, McEwen CN. 2010. Matrix-assisted laser desorption/ionization mass spectrometry method for selectively producing either singly or multiply charged molecular ions. *Anal. Chem.* 82:11–15
28. Van Berkel GJ, Pasilis SP, Ovchinnikova O. 2008. Established and emerging atmospheric pressure surface sampling/ionization techniques for mass spectrometry. *J. Mass Spectrom.* 43:1161–80
29. Venter A, Nefliu M, Graham Cooks RG. 2008. Ambient desorption ionization mass spectrometry. *Trends Anal. Chem.* 27:284–90
30. Chen H, Gamez G, Zenobi R. 2009. What can we learn from ambient ionization techniques? *J. Am. Soc. Mass Spectrom.* 20:1947–63
31. Covey TR, Thomson BA, Schneider BB. 2009. Atmospheric pressure ion sources. *Mass Spectrom. Rev.* 28:870–97
32. Alberici RM, Simas RC, Sanvido GB, Romão W, Lalli PM, et al. 2010. Ambient mass spectrometry: Bringing MS into the "real world." *Anal. Bioanal. Chem.* 398:265–94
33. Huang MZ, Yuan CH, Cheng SC, Cho YT, Shiea J. 2010. Ambient ionization mass spectrometry. *Annu. Rev. Anal. Chem.* 3:43–65

34. Weston DJ. 2010. Ambient ionization mass spectrometry: current understanding of mechanistic theory; analytical performance and application areas. *Analyst* 135:661–68
35. Harris GA, Galhena AS, Fernandez FM. 2011. Ambient sampling/ionization mass spectrometry: applications and current trends. *Anal. Chem.* 83:4508–38
36. Huang MZ, Cheng SC, Cho YT, Shiea J. 2011. Ambient ionization mass spectrometry: a tutorial. *Anal. Chim. Acta* 702:1–15
37. Nemes P, Vertes A. 2012. Ambient mass spectrometry for in vivo local analysis and in situ molecular tissue imaging. *Trends Anal. Chem.* 34:22–34
38. Wu C, Dill AL, Eberlin LS, Cooks RG, Ifa DR. 2012. Mass spectrometry imaging under ambient conditions. *Mass Spectrom. Rev.* 32:218–43
39. Badu-Tawiah AK, Eberlin LS, Ouyang Z, Cooks RG. 2013. Chemical aspects of the extractive methods of ambient ionization mass spectrometry. *Annu. Rev. Phys. Chem.* 64:481–505
40. Monge ME, Harris GA, Dwivedi P, Fernández FM. 2013. Mass spectrometry: recent advances in direct open air surface sampling/ionization. *Chem. Rev.* 113:2269–308
41. Ifa DR, Wu C, Ouyang Z, Cooks RG. 2010. Desorption electrospray ionization and other ambient ionization methods: current progress and preview. *Analyst* 135:669–81
42. Schilke DE, Levis RJ. 1994. A laser vaporization, laser ionization time-of-flight mass spectrometer for the probing of fragile biomolecules. *Rev. Sci. Instrum.* 65:1903–11
43. Brady JJ, Judge EJ, Levis RJ. 2009. Mass spectrometry of intact neutral macromolecules using intense non-resonant femtosecond laser vaporization with electrospray post-ionization. *Rapid Commun. Mass Spectrom.* 23:3151–57
44. DeWitt MJ, Levis RJ. 1995. Near-infrared femtosecond photoionization/dissociation of cyclic aromatic hydrocarbons. *J. Chem. Phys.* 102:8670–73
45. DeWitt MJ, Peters DW, Levis RJ. 1997. Photoionization/dissociation of alkyl substituted benzene molecules using intense near-infrared radiation. *Chem. Phys.* 218:211–23
46. Levis RJ, DeWitt MJ. 1999. Photoexcitation, ionization, and dissociation of molecules using intense near-infrared radiation of femtosecond duration. *J. Phys. Chem. A* 103:6493–507
47. Yang JJ, Gobeli DA, El-Sayed MA. 1985. Change in the mechanism of laser multiphoton ionization-dissociation in benzaldehyde by changing the laser pulse width. *J. Phys. Chem.* 89:3426–29
48. Weinkauf R, Aicher P, Wesley G, Grotemeyer J, Schlag E. 1994. Femtosecond versus nanosecond multiphoton ionization and dissociation of large molecules. *J. Phys. Chem.* 98:8381–91
49. Levis RJ, Menkir G, Rabitz H. 2001. Selective bond dissociation and rearrangement with optimally tailored, strong-field laser pulses. *Science* 292:709–13
50. Ledingham KWD, Smith DJ, Singhal RP, McCanny T, Graham P, et al. 1999. Multiply charged ions from aromatic molecules following irradiation in intense laser fields. *J. Phys. Chem. A* 103:2952–63
51. Odhner JH, Romanov DA, Levis RJ. 2009. Rovibrational wave-packet dispersion during femtosecond laser filamentation in air. *Phys. Rev. Lett.* 103:075005
52. Odhner JH, McCole ET, Levis RJ. 2011. Filament-driven impulsive Raman spectroscopy. *J. Phys. Chem. A* 115:13407–12
53. Bohinski T, Moore Tibbetts K, Tarazkar M, Romanov DA, Matsika S, Levis RJ. 2013. Measurement of an electronic resonance in ground state, gas phase acetophenone cation via strong field mass spectrometry. *J. Phys. Chem. Lett.* 4:1587–91
54. Arnolds H, Rehbein C, Roberts G, Levis RJ, King DA. 2000. Femtosecond near-infrared laser desorption of multilayer benzene on Pt{111}: a molecular Newton's cradle? *J. Phys. Chem. B* 104:3375–82
55. Arnolds H, Rehbein CE, Roberts G, Levis RJ, King DA. 1999. Femtosecond near-infrared laser desorption of multilayer benzene on Pt{111}: spatial origin of hyperthermal desorption. *Chem. Phys. Lett.* 314:389–95
56. Arnolds H, Levis RJ, King DA. 2003. Vibrationally assisted DIET through transient temperature rise: the case of benzene on Pt{111}. *Chem. Phys. Lett.* 380:444–50
57. Chichkov BN, Momma C, Nolte S, von Alvensleben F, Tünnermann A. 1996. Femtosecond, picosecond and nanosecond laser ablation of solids. *Appl. Phys. A* 63:109–15
58. Demirev P, Westman A, Reimann C, Håkansson P, Barofsky D, et al. 1992. Matrix-assisted laser desorption with ultra-short laser pulses. *Rapid Commun. Mass Spectrom.* 6:187–91

59. Wichmann J, Lupulescu C, Wöste L, Lindinger A. 2009. Matrix-assisted laser desorption/ionization by using femtosecond laser pulses in the near-infrared wavelength regime. *Rapid Commun. Mass Spectrom.* 23:1105–8
60. Van Breemen RB, Snow M, Cotter RJ. 1983. Time-resolved laser desorption mass spectrometry. I. Desorption of preformed ions. *Int. J. Mass Spectrom. Ion Phys.* 49:35–50
61. Russo RE, Mao X, Gonzalez JJ, Zorba V, Yoo J. 2013. Laser ablation in analytical chemistry. *Anal. Chem.* 85:6162–77
62. Brady JJ, Judge EJ, Levis RJ. 2010. *Laser electrospray mass spectrometry of adsorbed molecules at atmospheric pressure*. Presented at SPIE Photonics West Conf., San Francisco
63. Judge EJ, Brady JJ, Dalton D, Levis RJ. 2010. Analysis of pharmaceutical compounds from glass, fabric, steel, and wood surfaces at atmospheric pressure using spatially resolved, nonresonant femtosecond laser vaporization electrospray mass spectrometry. *Anal. Chem.* 82:3231–38
64. Judge EJ, Brady JJ, Levis RJ. 2010. Mass analysis of biological macromolecules at atmospheric pressure using nonresonant femtosecond laser vaporization and electrospray ionization. *Anal. Chem.* 82:10203–7
65. Brady JJ, Judge EJ, Levis RJ. 2011. Femtosecond laser vaporization of aqueous proteins with electrospray post-ionization preserves folded structure. *Proc. Natl. Acad. Sci. USA* 108:12217–22
66. Perez JJ, Flanigan PM, Karki S, Levis RJ. 2013. Laser electrospray mass spectrometry minimizes ion suppression facilitating quantitative mass spectral response for multicomponent mixtures of proteins. *Anal. Chem.* 85:6667–73
67. Brady JJ, Judge EJ, Levis RJ. 2011. Analysis of amphiphilic lipids and hydrophobic proteins using non-resonant femtosecond laser vaporization with electrospray post-ionization. *J. Am. Soc. Mass Spectrom.* 22:762–72
68. Judge EJ, Brady JJ, Barbano PE, Levis RJ. 2011. Nonresonant femtosecond laser vaporization with electrospray postionization for ex vivo plant tissue typing using compressive linear classification. *Anal. Chem.* 83:2145–51
69. Flanigan PM, Radell LL, Brady JJ, Levis RJ. 2012. Differentiation of eight phenotypes and discovery of potential biomarkers for a single plant organ class using laser electrospray mass spectrometry and multivariate statistical analysis. *Anal. Chem.* 84:6225–32
70. Sampson JS, Hawkridge AM, Muddiman DC. 2006. Generation and detection of multiply-charged peptides and proteins by matrix-assisted laser desorption electrospray ionization (MALDESI) Fourier transform ion cyclotron resonance mass spectrometry. *J. Am. Soc. Mass Spectrom.* 17:1712–16
71. Barry JA, Muddiman DC. 2011. Global optimization of the infrared matrix-assisted laser desorption electrospray ionization (IR MALDESI) source for mass spectrometry using statistical design of experiments. *Rapid Commun. Mass Spectrom.* 25:3527–36
72. Grandori R. 2003. Origin of the conformation dependence of protein charge-state distributions in electrospray ionization mass spectrometry. *J. Mass Spectrom.* 38:11–15
73. Flanigan PM, Perez JJ, Karki S, Levis RJ. 2013. Quantitative measurements of small molecule mixtures using laser electrospray mass spectrometry. *Anal. Chem.* 85:3629–37
74. Nemes P, Barton AA, Li Y, Vertes A. 2008. Ambient molecular imaging and depth profiling of live tissue by infrared laser ablation electrospray ionization mass spectrometry. *Anal. Chem.* 80:4575–82
75. Nemes P, Barton AA, Vertes A. 2009. Three-dimensional imaging of metabolites in tissues under ambient conditions by laser ablation electrospray ionization mass spectrometry. *Anal. Chem.* 81:6668–75
76. Pan P, McLuckey SA. 2003. Electrospray ionization of protein mixtures at low pH. *Anal. Chem.* 75:1491–99
77. Brady JJ, Judge EJ, Levis RJ. 2010. Identification of explosives and explosive formulations using laser electrospray mass spectrometry. *Rapid Commun. Mass Spectrom.* 24:1659–64
78. Brady JJ, Flanigan PM, Perez JJ, Judge EJ, Levis RJ. 2012. *Multidimensional detection of explosives and explosive signatures via laser electrospray mass spectrometry*. Presented at SPIE: Chemical, Biological, Radiological, Nuclear, and Explosives (CBRNE) Sensing XIII, Conf., Baltimore
79. Flanigan PM, Brady JJ, Judge EJ, Levis RJ. 2011. The determination of inorganic improvised explosive device signatures using laser electrospray mass spectrometry detection with offline classification. *Anal. Chem.* 83:7115–22

80. Perez JJ, Flanigan PM, Brady JJ, Levis RJ. 2013. Classification of smokeless powders using laser electrospray mass spectrometry and offline multivariate statistical analysis. *Anal. Chem.* 85:296–302
81. Shiea J, Huang MZ, Hsu HJ, Lee CY, Yuan CH, et al. 2005. Electrospray-assisted laser desorption/ionization mass spectrometry for direct ambient analysis of solids. *Rapid Commun. Mass Spectrom.* 19:3701–4
82. Huang MZ, Hsu HJ, Lee JY, Jeng J, Shiea J. 2006. Direct protein detection from biological media through electrospray-assisted laser desorption ionization/mass spectrometry. *J. Proteome Res.* 5:1107–16
83. Huang MZ, Jhang SS, Cheng CN, Cheng SC, Shiea J. 2010. Effects of matrix, electrospray solution, and laser light on the desorption and ionization mechanisms in electrospray-assisted laser desorption ionization mass spectrometry. *Analyst* 135:759–66
84. Huang MZ, Hsu HJ, Wu CI, Lin SY, Ma YL, et al. 2007. Characterization of the chemical components on the surface of different solids with electrospray-assisted laser desorption ionization mass spectrometry. *Rapid Commun. Mass Spectrom.* 21:1767–75
85. Shiea J, Chang DY, Lin CH, Jiang SJ. 2001. Generating multiply charged protein ions by ultrasonic nebulization/multiple channel-electrospray ionization mass spectrometry. *Anal. Chem.* 73:4983–87
86. Lee CC, Chang DY, Jeng J, Shiea J. 2002. Generating multiply charged protein ions via two-step electrospray ionization mass spectrometry. *J. Mass Spectrom.* 37:115–17
87. Shiea J, Wang CH. 1997. Applications of multiple channel electrospray ionization sources for biological sample analysis. *J. Mass Spectrom.* 32:247–50
88. Cheng SC, Lin YS, Huang MZ, Shiea J. 2010. Applications of electrospray laser desorption ionization mass spectrometry for document examination. *Rapid Commun. Mass Spectrom.* 24:203–8
89. Huang MZ, Cheng SC, Jhang SS, Chou CC, Cheng CN, et al. 2012. Ambient molecular imaging of dry fungus surface by electrospray laser desorption ionization mass spectrometry. *Int. J. Mass Spectrom.* 325–27:172–82
90. Lin SY, Huang MZ, Chang HC, Shiea J. 2007. Using electrospray-assisted laser desorption/ionization mass spectrometry to characterize organic compounds separated on thin-layer chromatography plates. *Anal. Chem.* 79:8789–95
91. Cheng SC, Huang MZ, Wu LC, Chou CC, Cheng CN, et al. 2012. Building blocks for the development of an interface for high-throughput thin layer chromatography/ambient mass spectrometric analysis: a green methodology. *Anal. Chem.* 84:5864–68
92. Shiea J, Yuan CH, Huang MZ, Cheng SC, Ma YL, et al. 2008. Detection of native protein ions in aqueous solution under ambient conditions by electrospray laser desorption/ionization mass spectrometry. *Anal. Chem.* 80:4845–52
93. Peng IX, Shiea J, Ogorzalek Loo RR, Loo JA. 2007. Electrospray-assisted laser desorption/ionization and tandem mass spectrometry of peptides and proteins. *Rapid Commun. Mass Spectrom.* 21:2541–46
94. Cheng CY, Yuan CH, Cheng SC, Huang MZ, Chang HC, et al. 2008. Electrospray-assisted laser desorption/ionization mass spectrometry for continuously monitoring the states of ongoing chemical reactions in organic or aqueous solution under ambient conditions. *Anal. Chem.* 80:7699–705
95. Peng IX, Ogorzalek Loo RR, Shiea J, Loo JA. 2008. Reactive-electrospray-assisted laser desorption/ionization for characterization of peptides and proteins. *Anal. Chem.* 80:6995–7003
96. Peng IX, Ogorzalek Loo RR, Margalith E, Little MW, Loo JA. 2010. Electrospray-assisted laser desorption ionization mass spectrometry (ELDI-MS) with an infrared laser for characterizing peptides and proteins. *Analyst* 135:767–72
97. Nemes P, Vertes A. 2007. Laser ablation electrospray ionization for atmospheric pressure, in vivo, and imaging mass spectrometry. *Anal. Chem.* 79:8098–106
98. Sampson JS, Murray KK, Muddiman DC. 2009. Intact and top-down characterization of biomolecules and direct analysis using infrared matrix-assisted laser desorption electrospray ionization coupled to FT-ICR, mass spectrometry. *J. Am. Soc. Mass Spectrom.* 20:667–73
99. Dixon RB, Sampson JS, Hawkridge AM, Muddiman DC. 2008. Ambient aerodynamic ionization source for remote analyte sampling and mass spectrometric analysis. *Anal. Chem.* 80:5266–71
100. Dixon RB, Muddiman DC. 2010. Study of the ionization mechanism in hybrid laser based desorption techniques. *Analyst* 135:880–82

101. Dixon RB. 2009. *The development and utilization of aerodynamic devices in biological mass spectrometry*. PhD thesis, N.C. State Univ., Raleigh
102. Sampson JS, Hawkridge AM, Muddiman DC. 2008. Development and characterization of an ionization technique for analysis of biological macromolecules: liquid matrix-assisted laser desorption electrospray ionization. *Anal. Chem.* 80:6773–78
103. König S, Kollas O, Dreisewerd K. 2007. Generation of highly charged peptide and protein ions by atmospheric pressure matrix-assisted infrared laser desorption/ionization ion trap mass spectrometry. *Anal. Chem.* 79:5484–88
104. Sampson JS, Hawkridge AM, Muddiman DC. 2007. Direct characterization of intact polypeptides by matrix-assisted laser desorption electrospray ionization quadrupole Fourier transform ion cyclotron resonance mass spectrometry. *Rapid Commun. Mass Spectrom.* 21:1150–54
105. Cochran KH, Barry JA, Muddiman DC, Hinks D. 2013. Direct analysis of textile fabrics and dyes using infrared matrix-assisted laser desorption electrospray ionization mass spectrometry. *Anal. Chem.* 85:831–36
106. Robichaud G, Barry JA, Garrard KP, Muddiman DC. 2013. Infrared matrix-assisted laser desorption electrospray ionization (IR-MALDESI) imaging source coupled to a FT-ICR mass spectrometer. *J. Am. Soc. Mass Spectrom.* 24:92–100
107. Barry JA, Robichaud G, Muddiman DC. 2013. Mass recalibration of FT-ICR mass spectrometry imaging data using the average frequency shift of ambient ions. *J. Am. Soc. Mass Spectrom.* 24:1137–45
108. Laiko VV, Taranenko NI, Berkout VD, Yakshin MA, Prasad CR, et al. 2002. Desorption/ionization of biomolecules from aqueous solutions at atmospheric pressure using an infrared laser at 3 μm. *J. Am. Soc. Mass Spectrom.* 13:354–61
109. Dreisewerd K. 2003. The desorption process in MALDI. *Chem. Rev.* 103:395–426
110. Dreisewerd K, Berkenkamp S, Leisner A, Rohlfing A, Menzel C. 2003. Fundamentals of matrix-assisted laser desorption/ionization mass spectrometry with pulsed infrared lasers. *Int. J. Mass Spectrom.* 226:189–209
111. Apitz I, Vogel A. 2005. Material ejection in nanosecond Er:YAG laser ablation of water, liver, and skin. *Appl. Phys. A* 81:329–38
112. Chen Z, Bogaerts A, Vertes A. 2006. Phase explosion in atmospheric pressure infrared laser ablation from water-rich targets. *Appl. Phys. Lett.* 89:041503
113. Chen Z, Vertes A. 2008. Early plume expansion in atmospheric pressure midinfrared laser ablation of water-rich targets. *Phys. Rev. E* 77:036316
114. Jackson SN, Kim JK, Laboy JL, Murray KK. 2006. Particle formation by infrared laser ablation of glycerol: implications for ion formation. *Rapid Commun. Mass Spectrom.* 20:1299–304
115. Musapelo T, Murray KK. 2011. Particle formation in ambient MALDI plumes. *Anal. Chem.* 83:6601–8
116. Fan X, Little MW, Murray KK. 2008. Infrared laser wavelength dependence of particles ablated from glycerol. *Appl. Surf. Sci.* 255:1699–704
117. Protea Biosciences. 2014. The *LAESI DP-1000 System is a high-throughput direct ionization system that profiles the distribution of biomolecules.* Morgantown, WV, retrieved 2/18/14. **https://proteabio.com/LAESI?state=laesi**
118. Nemes P, Huang H, Vertes A. 2012. Internal energy deposition and ion fragmentation in atmospheric-pressure mid-infrared laser ablation electrospray ionization. *Phys. Chem. Chem. Phys.* 14:2501–7
119. Nemes P, Woods AS, Vertes A. 2010. Simultaneous imaging of small metabolites and lipids in rat brain tissues at atmospheric pressure by laser ablation electrospray ionization mass spectrometry. *Anal. Chem.* 82:982–88
120. Shrestha B, Vertes A. 2009. In situ metabolic profiling of single cells by laser ablation electrospray ionization mass spectrometry. *Anal. Chem.* 81:8265–71
121. Shrestha B, Nemes P, Vertes A. 2010. Ablation and analysis of small cell populations and single cells by consecutive laser pulses. *Appl. Phys. A* 101:121–26
122. Shrestha B, Patt JM, Vertes A. 2011. In situ cell-by-cell imaging and analysis of small cell populations by mass spectrometry. *Anal. Chem.* 83:2947–55
123. Sripadi P, Shrestha B, Easley R, Carpio L, Kehn-Hall K, et al. 2011. Direct detection of diverse metabolic changes in virally transformed and tax-expressing cells by mass spectrometry. *PLoS ONE* 5:e12590

124. Shrestha B, Sripadi P, Walsh CM, Razunguzwa TT, Powell MJ, et al. 2012. Rapid, non-targeted discovery of biochemical transformation and biomarker candidates in oncovirus-infected cell lines using LAESI mass spectrometry. *Chem. Commun.* 48:3700–2
125. Parsiegla G, Shrestha B, Carrière F, Vertes A. 2011. Direct analysis of phycobilisomal antenna proteins and metabolites in small cyanobacterial populations by laser ablation electrospray ionization mass spectrometry. *Anal. Chem.* 84:34–38
126. Stolee JA, Vertes A. 2013. Toward single cell analysis by plume collimation in laser ablation electrospray ionization mass spectrometry. *Anal. Chem.* 85:3592–98
127. Vaikkinen A, Shrestha B, Nazarian J, Kostiainen RK, Vertes A, Kauppila TJ. 2013. Simultaneous detection of nonpolar and polar compounds by heat-assisted laser ablation electrospray ionization-mass spectrometry. *Anal. Chem.* 85:177–84
128. Vaikkinen A, Shrestha B, Kauppila TJ, Vertes A, Kostiainen R. 2012. Infrared laser ablation atmospheric pressure photoionization mass spectrometry. *Anal. Chem.* 84:1630–36
129. Fernandez de la Mora J. 2011. Ionization of vapor molecules by an electrospray cloud. *Int. J. Mass Spectrom.* 300:182–93
130. Rezenom YH, Dong J, Murray KK. 2007. Infrared laser-assisted desorption electrospray ionization mass spectrometry. *Analyst* 133:226–32
131. Harris GA, Graf S, Knochenmuss R, Fernandez F. 2012. Coupling laser ablation/desorption electrospray ionization to atmospheric pressure drift tube ion mobility spectrometry for the screening of antimalarial drug quality. *Analyst* 137:3039–44
132. Sampson JS, Muddiman DC. 2009. Atmospheric pressure infrared (10.6 μm) laser desorption electrospray ionization (IR-LDESI) coupled to a LTQ Fourier transform ion cyclotron resonance mass spectrometer. *Rapid Commun. Mass Spectrom.* 23:1989–92
133. Jorabchi K, Smith LM. 2009. Single droplet separations and surface partition coefficient measurements using laser ablation mass spectrometry. *Anal. Chem.* 81:9682–88
134. Liu J, Qiu B, Luo H. 2010. Fingerprinting of yogurt products by laser desorption spray post-ionization mass spectrometry. *Rapid Commun. Mass Spectrom.* 24:1365–70
135. Liu J, Zhang C, Sun J, Luo H. 2012. Unexpected complexation reaction during analysis of proteins using laser desorption spray post-ionization mass spectrometry. *Analyst* 137:1764–67
136. Liu J, Zhang C, Sun J, Ren X, Luo H. 2013. Laser desorption dual spray post-ionization mass spectrometry for direct analysis of samples via two informative channels. *J. Mass Spectrom.* 48:250–54
137. Ovchinnikova OS, Kertesz V, Van Berkel GJ. 2011. Combining laser ablation/liquid phase collection surface sampling and high-performance liquid chromatography–electrospray ionization-mass spectrometry. *Anal. Chem.* 83:1874–78
138. Ovchinnikova OS, Kertesz V, Van Berkel GJ. 2011. Combining transmission geometry laser ablation and a non-contact continuous flow surface sampling probe/electrospray emitter for mass spectrometry based chemical imaging. *Rapid Commun. Mass Spectrom.* 25:3735–40
139. Park SG, Murray KK. 2011. Infrared laser ablation sample transfer for MALDI and electrospray. *J. Am. Soc. Mass Spectrom.* 22:1352–62
140. Park SG, Murray KK. 2012. Infrared laser ablation sample transfer for on-line liquid chromatography electrospray ionization mass spectrometry. *J. Mass Spectrom.* 47:1322–26
141. Park SG, Murray KK. 2013. Ambient laser ablation sampling for capillary electrophoresis mass spectrometry. *Rapid Commun. Mass Spectrom.* 27:1673–80
142. Kaufman E, Smith W, Kowalski M, Beech I, Sunner J. 2013. Electric-field-enhanced collection of laser-ablated materials onto a solvent bridge for electrospray ionization mass spectrometry. *Rapid Commun. Mass Spectrom.* 27:1567–72
143. Cheng SC, Cheng TL, Chang HC, Shiea J. 2009. Using laser-induced acoustic desorption/electrospray ionization mass spectrometry to characterize small organic and large biological compounds in the solid state and in solution under ambient conditions. *Anal. Chem.* 81:868–74
144. Cheng SC, Huang MZ, Shiea J. 2009. Thin-layer chromatography/laser-induced acoustic desorption/electrospray ionization mass spectrometry. *Anal. Chem.* 81:9274–81

145. Trimpin S, Inutan ED, Herath TN, McEwen CN. 2010. Laserspray ionization, a new atmospheric pressure MALDI method for producing highly charged gas-phase ions of peptides and proteins directly from solid solutions. *Mol. Cell Proteomics* 9:362–67
146. Inutan ED, Wang B, Trimpin S. 2011. Commercial intermediate pressure MALDI ion mobility spectrometry mass spectrometer capable of producing highly charged laserspray ionization ions. *Anal. Chem.* 83:678–84
147. Inutan ED, Wager-Miller J, Mackie K, Trimpin S. 2012. Laserspray ionization imaging of multiply charged ions using a commercial vacuum MALDI ion source. *Anal. Chem.* 84:9079–84
148. Trimpin S, Ren Y, Wang B, Lietz CB, Richards AL, et al. 2011. Extending the laserspray ionization concept to produce highly charged ions at high vacuum on a time-of-flight mass analyzer. *Anal. Chem.* 83:5469–75
149. McEwen CN, Larsen BS, Trimpin S. 2010. Laserspray ionization on a commercial atmospheric pressure-MALDI mass spectrometer ion source: selecting singly or multiply charged ions. *Anal. Chem.* 82:4998–5001
150. McEwen CN, Trimpin S. 2011. An alternative ionization paradigm for atmospheric pressure mass spectrometry: flying elephants from Trojan horses. *Int. J. Mass Spectrom.* 300:167–72
151. Trimpin S, Wang B, Inutan ED, Li J, Lietz CB, et al. 2012. A mechanism for ionization of nonvolatile compounds in mass spectrometry: considerations from MALDI and inlet ionization. *J. Am. Soc. Mass Spectrom.* 23:1644–60
152. Inutan E, Trimpin S. 2010. Laserspray ionization (LSI) ion mobility spectrometry (IMS) mass spectrometry. *J. Am. Soc. Mass Spectrom.* 21:1260–64
153. Inutan ED, Trimpin S. 2010. Laserspray ionization-ion mobility spectrometry–mass spectrometry: baseline separation of isomeric amyloids without the use of solvents desorbed and ionized directly from a surface. *J. Proteome Res.* 9:6077–81
154. Richards AL, Lietz CB, Wager-Miller JB, Mackie K, Trimpin S. 2011. Imaging mass spectrometry in transmission geometry. *Rapid Commun. Mass Spectrom.* 25:815–20
155. Inutan ED, Richards AL, Wager-Miller J, Mackie K, McEwen CN, Trimpin S. 2011. Laserspray ionization, a new method for protein analysis directly from tissue at atmospheric pressure with ultrahigh mass resolution and electron transfer dissociation. *Mol. Cell Proteomics* 10:1–8
156. Ren X, Liu J, Zhang C, Luo H. 2013. Direct analysis of samples under ambient condition by high-voltage-assisted laser desorption ionization mass spectrometry in both positive and negative ion mode. *Rapid Commun. Mass Spectrom.* 27:613–20
157. Schäfer KC, Szaniszló T, Günther S, Balog J, Dénes J, et al. 2011. In situ, real-time identification of biological tissues by ultraviolet and infrared laser desorption ionization mass spectrometry. *Anal. Chem.* 83:1632–40
158. Coello Y, Jones AD, Gunaratne TC, Dantus M. 2010. Atmospheric pressure femtosecond laser imaging mass spectrometry. *Anal. Chem.* 82:2753–58